PARAMETER-BASED OPTIMAL DESIGN OF AN IE4 CLASS INDUCTION MOTOR

BURÇAK MELİS BULUÇ BİLLUR

FEBRUARY 2024

ÇANKAYA UNIVERSITY

GRADUATE SCHOOL OF NATURAL AND APPLIED SCIENCES

DEPRTMENT F ELECTRICAL AND ELECTRONICS ENGINEERING

M.Sc. Thesis in

ELECTRICAL AND ELECTRONICS ENGINEERING

PARAMETER-BASED OPTIMAL DESIGN OF AN IE4 CLASS INDUCTION MOTOR

BURÇAK MELİS BULUÇ BİLLUR

FEBRUARY 2024

ABSTRACT

PARAMETER-BASED OPTIMAL DESIGN OF AN IE4 CLASS INDUCTION MOTOR

BULUÇ BİLLUR, Burçak Melis
M.Sc. in Electrical and Electronics Engineering

Supervisor: Prof. Dr. İres İSKENDER
Co-Supervisor: Assist. Prof. Dr. Cemil OCAK
February 2024, 91 pages

Induction motors have a wide range of applications in the industrial field. The use of high efficiency motors has become increasingly important with the development of technology, surpassing the significance of standard efficient motors. This shift has resulted in significant positive developments in terms of energy consumption. In order to achieve energy efficiency savings, motor technology has undergone significant development. Recent studies have focused on improving the efficiency of induction motors. The results show a significant increase in induction motor efficiency. This study implements a new design that emphasizes parameters such as stator and rotor slot design, winding design, and stack length determination, while taking into account cost constraints.

This thesis outlines the acquisition of a 110 kW squirrel cage induction motor with high efficiency and IE4 efficiency class, which demonstrates our commitment to sustainability and energy efficiency. The thesis consists of 6 chapters. Chapter I of this thesis provides comprehensive information on electric motors, including their operational principles, areas of application, and accessories. Chapter II outlines the relevant formulas for designing the electric motor, Chapter III details efficiency regulation, Chapter IV presents the design analysis results of the selected reference motor, Chapter V includes the design criteria, analysis, and official test results of the

newly designed motor, and Chapter VI discusses the study results and potential future designs.

Keywords: Cost Optimization, Efficiency, IE4, Induction Motor Design, Loss, Parameter Design Optimization

ÖZET

IE4 SINIFI BİR ASENKRON MOTORUN PARAMETRE TABANLI OPTİMUM TASARIMI

BULUÇ BİLLUR, Burçak Melis
Elektrik-Elektronik Mühendisliği Yüksek Lisans

Danışman: Prof. Dr. İres İSKENDER
Ortak Danışman: Dr. Öğr. Üyesi Cemil OCAK
Şubat 2024, 91 sayfa

İndüksiyon motorların çok geniş yelpazesi vardır ve endüstriyel alanda büyük bir kullanıma sahiptir. Günümüzde gelişen teknolojiyle birlikte standart verimli motorların kullanılması azaltılıp yüksek verimli motorların kullanılması daha büyük önem arz etmiştir. Bu nedenle yüksek verimli motorların kullanılması enerji tüketim açısından daha olumlu gelişmelere vesile olmuştur. Enerji verimliliği açısından tasarruf elde edebilmek için motor teknoloji gelişmiş ve son yapılan çalışmalar ise indüksiyon motorların verimliliği üzerine olmuştur. Bu nedenle, bu çalışmada indüksiyon motorun verimi arttırabilmek amacıyla yeni bir tasarım icra edilmiştir. Maliyet kısıtı göz önüne alınıp, stator ve rotor oluk tasarımı, sargı tasarımı, paket boyu belirleme gibi bir çok parametre üzerine durulmuştur.

Bu tez çalışmasında 110 kW gücünde sincap kafesli IE4 verim sınıfına sahip yüksek verimli indüksiyon motoru elde edilmiştir.

Tez 6 bölümden oluşmaktadır: Bu tezin I. Bölümü, çalışma prensipleri, uygulama alanları ve aksesuarları da dahil olmak üzere elektrik motorları hakkında kapsamlı bilgi vermektedir. Bölüm II'de elektrik motoru tasarımı için ilgili formüller özetlenmekte, Bölüm III'te verimlilik düzenlemesi detaylandırılmakta, Bölüm IV'te seçilen referans motorun tasarım analizi sonuçları sunulmakta, Bölüm V'te yeni

tasarlanan motorun tasarım kriterleri, analizi ve resmi test sonuçları yer almakta ve Bölüm VI'da çalışma sonuçları ve gelecekteki potansiyel tasarımlar tartışılmaktadır.

Anahtar Kelimeler: Maliyet Optimizasyonu, Verimlilik, IE4, İndüksiyon Motor Tasarımı, Kayıp, Parametre Dizayn Optimizasyonu

ACKNOWLEDGEMENT

I would like to express my respect and gratitude to my esteemed teacher Prof. Dr. İres İSKENDER and Asst. Prof. Dr. Cemil OCAK for their valuable contributions towards my academic endeavors. I would like to express my gratitude to Şakir KINACI for tirelessly sharing his knowledge of electric motors with me, answering all my questions, and providing moral support. I would also like to thank Elsan Elektrik San.ve. Tic.AŞ. and my colleagues for their assistance in producing and testing my electric motor designs. I would like to express my gratitude to Ceyhun ERMAN for his support in commencing my master's degree, Barış ERDOĞAN for his assistance in producing the electric motor, as well as Gürhan HANİF and Muratcan ÖZTÜRK for their support in using the company's facilities. I would like to express my gratitude to my family for their unwavering love and support. Specifically, I would like to thank my mother, Zekiye BULUÇ, my father, Naci BULUÇ, and my brother, Burak BULUÇ.

Additionally, I am grateful for the support and encouragement of my husband, Mustafa Eray BİLLUR, who provided both financial and emotional support throughout my academic journey. Without his help, I would not have been able to complete my thesis.

I would like to express my gratitude to my dear friend Hüseyin Basri ÇERÇİ, who provided invaluable assistance and unwavering support throughout this process. Thank you all for your support.

TABLE OF CONTENTS

LIST OF TABLES

LIST OF FIGURES

LIST OF SYMBOLS AND ABBREVIATIONS

Symbols

$H = \frac{B}{\mu}$	: Magnetic Field Strength
$\vec{J} = \sigma\vec{E}$	: Current Strength
$\vec{B}$	: Magnetic Flux Density
ϕ_B	: Magnetic Flux
f_s	: Stator Frequency
n_r	: Rotor Slip
n_s	: Stator Slip
η	: Efficiency
Bs0 [mm]	: Slot Lower Width
Bs1 [mm]	: Slot Lower Width
Bs2 [mm]	: Slot Upper Width
Cosø	: Power Factor
f	: Frequency
Hs0 [mm]	: Slot Mouth Height
Hs01 [mm]	: Slot Airgap Length
Hs1 [mm]	: Radius
Hs2 [mm]	: Slot Height
I	: Current
Ik	: Inrush current
In	: Rated current
Mk	: Starting torque
Mn	: Nominal Moment
p	: Pole Number
P1	: Input Power
P1ϑ	: Corrected Input Power
P2	: Output Power

P2 (kW)	: Additional Losses 0,5 % From Pn Acc.
Pcu1 (kW)	: Stator Copper Losses
Pcu2 (kW)	: Rotor Conductor Losses
Pd (kW)	: Power In Air Gap Between Stator and Rotor
Pfe (kW)	: Iron Losses
Pmech (kW)	: Mechanical Losses
Pr ϑ	: Corrected Rotor Losses
Protor (kW)	: Total Rotor Losses
Ps ϑ	: Corrected Stator Losses
Pstat (kW)	: Total Stator Losses
Ptot (kW)	: Total Motor Losses
R	: Resistance
Rt K	: Rotor Temperature
RT Ø	: Rotor Outer Diameter
s	: Slip
St K	: Stator Temperature
ST Ø	: Stator Outer Diameter
T	: Torque
U	: Voltage

Abbreviations

BEIS	: Business, Energy & Industrial Strategy
CEMEP	: European Committee of Manufacturers of Electrical Machines and Power Electronics
EC	: European Community
FEM	: Finite Element Method
IE1	: Standard Efficiency Motors
IE2	: High Efficiency Motors
IE3	: Premium Efficient Motors
IE4	: Super Premium Efficient Motors
IEC	: International Electrotechnical Commission
LSPMSM	: Low Speed Permanent Magnet
NEMA	: National Electrical Manufacturers Association

SynRM : Synchronous Reluctance Machine

TSE : Turkish Standards Institute

CHAPTER I
INTRODUCTION

1.1 AIM AND OBJECTIVES

When designing an electric motor, it is crucial to carefully select the motor components, calculate the optimal winding numbers, determine the stator and rotor slot dimensions, and choose the appropriate mechanical and insulation materials. By taking all of these factors into account, a well-designed electric motor can be created that meets the needs of the intended application. It is important to consider factors such as efficiency, reliability, size, weight, cost, and suitability for specific operating conditions. In order to manage expenses, the cooling systems have been optimized to minimize motor losses. A variety of methodologies and innovative approaches are utilized to consistently enhance the efficiency and performance of electric motor design.

Chapter I of this thesis provides comprehensive information on electric motors, including their operational principles, areas of application, and accessories. Chapter II outlines the relevant formulas for designing the electric motor, Chapter III details efficiency regulation, Chapter IV presents the design analysis results of the selected reference motor, Chapter V includes the design criteria, analysis, and official test results of the newly designed motor, and Chapter VI discusses the study results and potential future designs.

1.2 LITERATURE SURVEY

Several investigations have been conducted in the literature on electric motor design to determine the most appropriate design for different objectives. Optimization studies have been carried out on various parameters to determine the design purpose and results. Several metaheuristic algorithms have been employed to conduct these optimization studies. In certain instances, the optimization results have been corroborated by analysis findings. These motors thus have a key role in the industrial sector due to their high energy efficiency. These motors make a valuable contribution

to energy conservation and the achievement of sustainable environmental objectives. Nevertheless, on account of their elevated cost, their deployment may lessen their appeal.

A.R. Gallego explores the design and optimization studies executed to reach the IE4 level of efficiency for a 4-pole, 7.5 kW motor. The methods used to reduce motor losses were emphasized, along with a discussion of the studies carried out on the existing lamination. The first part of the thesis provides an overview of the types of losses, calculation methods and loss analysis formulas. Examples demonstrating potential optimization through equations are presented whereby results from various studies are shared through evaluations and performance testing. The dissertation includes an analysis of the impact of certain factors such as rotor active material, slot fill factor, stack length, steel type used, and increased slot cross-sections on motor efficiency. Following the study, it was suggested that copper be utilized for the rotor slots and end ring in order to achieve an IE4 efficiency level. Additionally, the existing aluminum bars and end rings could enhance the efficiency level by enlarging the rotor and stator slots regions [1].

In L. R. Middelberg's paper, he presented information on motor and system efficiency. In his study, he emphasised that thinner sheet laminations should be used to reduce magnetic circuit losses. It is suggested that the efficiency of the machine can be improved by modifying the stator diameter and stack length as well as the stator tooth between the two slots. This is due to the fact that larger stator slots may lead to magnetic saturation and increased losses. At the same time, it is indicated that altering the stator may also affect the machine's torque. Additionally, it is emphasized that increasing resistance will result in an increase in slip for the same level of moment. For the same torque value, the rotor's speed will be lower with a larger resistance. When slip is low, the speed increases, but as the rotation speed of the fan increases, friction losses also increase [2].

Ioan Peter's examines the factors impacting motor efficiency through mathematical equations and proposes methods for reducing losses and improving efficiency up to the IE2 level for motors up to 18.5 kW. The paper mentions the significance of cost in new lamination (slot) design and sizing, particularly at the outset of these methods. Due to the high investment, mould, frame, and end bell mould costs, the focus shifted to potential improvements to the current system. Core losses and additional losses were the major area of concentration, with explanations provided

through mathematical expressions. The writer explained hysteresis and eddy current losses (also referred to as foucault) using mathematical equations. To decrease iron losses in the core, it is recommended to use steel sheets with a lower loss coefficient. The process of laminating, which involves the use of cutters and dies on machines, can significantly affect the shape of the stator. This can result in increased iron losses.To prevent this, it is recommended that printing machines use the most sensitive equipment available. Additionally, lathe should not be applied to the stator after the printing process. It is argued that lamination during the turning process has a direct impact on flux distribution and reduces efficiency. Four additional losses are analyzed and categorized, including surface losses and losses of surface between the rotor bars. It is noted that the effect of transverse currents is greater. Transverse currents that flow in the rotor increase the surface resistance while reducing the impact of currents and surface losses for optimal utilization. If the rotor slots are not insulated with lamination, the current between the rotor rods will flow not only in the end ring, but also through the lamination, leading to additional losses. To increase the surface resistance, it is recommended to perform thermal shocking on the rotor, which will effectively raise the resistance. The experiments indicate an enhanced motor efficiency. Surface resistance increase results in a reduction of rotor aluminum losses, motor starting current, locked rotor input power, and an increase in starting torque. The production process may contribute to the decrease in starting current and the increase in starting torque, which significantly impacts efficiency. The study highlights the impact of the air gap on motor parameters. It suggests that reducing the air gap results in an increase in magnetic field density and power factor, thereby enhancing efficiency. Furthermore, a decrease in the air gap leads to a reduction in starting current and starting torque [3].

Cui Shumei and colleagues conducted a study on the design of rotor slots. The study aimed to explore the impact of rotor design on motor torque performance and noise. To this end, three distinct rotor slot designs were proposed and analyzed in terms of their efficiency, losses, torque response, and noise [4].

Eveline Makhetha et al. conducted research on the effects of rotor bar shapes on the efficiency and power factor, as well as the impact of stator slot width on the performance of 3-phase induction motor using Finite Element Modelling. Their findings show that the most efficient results are achieved with unsharpened corners [5].

Yuanfeng Huang and Haifeng Wang conducted research on stator and they studied the effect of the number of stator windings and the tilt angle on the motor performance. They used mathematical expressions to explain their findings.They found that increasing the number of stator windings or utilizing a deep and narrow slot structure suppressed harmonic currents and improved the power factor. They observed that efficiency increased with the optimal design of stator and rotor inclination angles.At the same time, the researchers reached experimental conclusions by providing comprehensive details of the stator slot type and rotor designs [6].

Ashwin D. et al. found that incorporating high-quality materials and using copper instead of aluminum in the rotor resulted in increased efficiency. They also observed that augmenting the core length and improving the windings positively impacted the efficiency of the IE4 motor they optimized [7].

Dianhai Zhang, Ziyan Ren and Chang-Seop Koh utilised mathematical expressions to evaluate efficiency in their research. They determined the torque-speed characteristics and optimised them to identify the most suitable rotor slot shapes. Subsequently, performance evaluations were conducted via FEM analysis. The algorithm proved valuable in augmenting efficiency and power factor values whilst simultaneously reducing costs [8].

C.Saravanan and his students found that modifying the stator windings resulted in improved efficiency and power factor, while also reducing stator and rotor losses. The adjustments led to increased efficiency and power factor, along with a decrease in stator and rotor losses. Additionally, they utilized MATLAB SIMULINK to create a mathematical model of the motor simulation [9].

In their article "Manufacturing of IE4 induction motors," Catalin Petrea Ion and Ioan Peter devised mathematical models for motor losses in order to enhance motor efficiency. They managed to increase efficiency by 1.5% in their prototypes by decreasing the number of turns in the windings and increasing the wire diameter. In addition, they elongated the stack length and core diameter and incorporated silicon sheet metal with lower losses. The authors recommended rewinding the motor and extending the stack length as the most affordable options. The authors recommended rewinding the motor and extending the stack length as the most affordable options [10]. For instance, one thesis study examined solely the impact of the rotor's geometric data on efficiency, while another focused on developing the winding design. Other studies provided information on the casting material of the rotor or the effect of

changing stack lengths on efficiency, although the latter did not yield sufficient improvement to be included in this thesis study. Therefore, this thesis reviews all parameters that can improve efficiency and presents a new design that achieves IE4 efficiency. The parameters for the complete system design have been improved with the aforementioned enhancements.

1.3 AIM OF THESIS

This thesis investigates the design of an induction motor that complies with IE4 efficiency standards from a broad perspective. The structure is clear, with a logical progression and causal connections between statements. The study aims to achieve the high efficiency levels required by the IE4 standard through the optimization of stator and rotor slots, windings, and other parameters in the design of electric motors.We have established specific objectives within this framework to achieve our main goals: the objective is to develop strategies that reduce material usage and design processes to achieve IE4 efficiency. The emphasis should be on green energy and environmentally friendly methods to ensure compliance with sustainability principles. Furthermore, the design must adhere to industry standards and anticipated technological advancements. The aim is to create a durable, high-performance, and highly efficient motor that balances performance and longevity.

CHAPTER II
ELECTRIC MOTORS

2.1 HISTORY OF ELECTRIC MOTORS

Invention of Faraday about the electromagnetism in 1831, initiate to development of electric machines. From mechanical energy to electrical energy in electric generator and from electrical energy to mechanical motion are based on Faraday's law [11,12]. This invention affected our daily life in very aspects. After the discovery of Faraday, Rutland Vermont produced the first ever electric motor in Devenport [12]. This particular motor is the first direct current (DC) motor in the history. First ever alternating current (AC) motor was invented by Nikola Tesla in 1888. With the invention of AC motors, family of generic electric motors was completed [12]. However, invention of AC motors was immense, many refinements on these motors are made by engineers in last few decades, and brushless DC, stepper, and servo motors were invented.

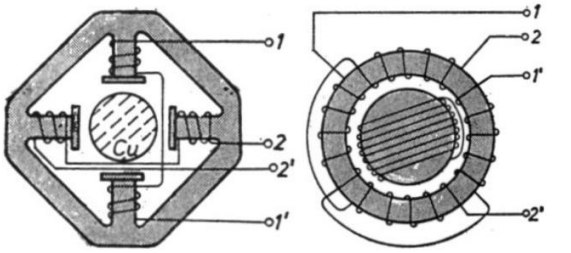

(a) Galileo Ferraris patent (b) Nicola Tesla patent (1886)

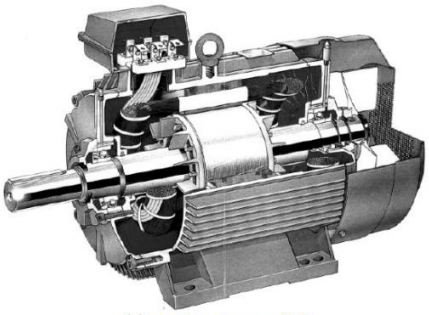

(c) contemporary IM

Figure 2.1: Induction Motors. (a) Galileo Ferraris Patent;(b) Nicola Tesla Patent (1886); (c) Contemporary IM

Between 1861 and 1864, James Clark Maxwell summarized the present understanding of electromagnetism in four fundamental equations. These equations remain valid today and provide a complete description of electrical engineering theory [13]. Siemens developed the dynamo-electric machine based on the "double T" armature between 1866 and 1867. Ultimately, during this timeframe, a potent electric generator was deployed, allowing the unimpeded flow of electricity [3]. In 1871, Zénobe Théophil Gramme, a Belgian inventor, resolved the challenge of generating a pulsed direct current in Siemens' T-armature dynamoelectric machine by using an iron ring. While initially a serious competitor to Siemens, this technology is no longer in use [13]. Between 1871 and 1875, Friedrich von Hefner-Alteneck, a German and assistant to Werner Siemens, began development on the drum motor. He began his work by coiling wire around a cylindrical iron and created a double T-ring machine with the ability to produce direct voltage. He then established new models aimed at increasing efficiency and produced prototypes of the new designs. These prototypes underwent performance tests, and the analysis and test results were compared. In 1875, he replaced the solid iron core with thin iron sheets to reduce eddy currents [13]. In 1873, Auguste Pellerin, a Frenchman, proposed dividing the iron core into multiple mutually insulated steel plates to prevent eddy current losses. However, the concept remained at the idea stage. During the same period, Ritchie invented the commutator and laid the groundwork for constructing the DC motor. Although various inventors such as Jedlik, Jacobi, Davenport, Davidson, and Page worked on and developed the DC motor in subsequent years, the foundation of the DC machine is credited to the dynamo machine devised by Siemens [13]. During the period of 1882 to 1889, the three-phase system and induction motor underwent development. While studying in Austria, Nicola Tesla was contemplating a multiphase voltage system. In 1884, he migrated to America and established a small company's development laboratory in New York by 1886. In 1885, Italian Professor Ferraris successfully built a small two-phase induction motor. Soon after, Tesla invented the two-phase motor, without any knowledge of Ferraris' work, and developed a range of functional models [13]. Tesla continued his work, alongside his investors, for two years until 1887 when he received his first patent for the first two-phase four-power cable AC system. Tesla captured George Westinghouse's interest with his speech at the American Engineering Institute in Pittsburgh in May 1888 and proceeded to sell more than 40 patents to Westinghouse for 1 million pounds. As a result, Tesla became a consultant to Westinghouse. During

his tenure at Westinghouse, he focused on relatively high frequency two-phase and single-phase AC systems [13].In recent years, research on the energy efficiency of electrical machines has become widespread. In 2014, electric motors consume about 40% of the world's electricity and more than 70% of industrial electricity [15]. On the other hand, these motors generate nearly the 13% of global carbon emission [14].

This field typically examines subjects including the design and analysis of energy-efficient motors, industrial applications of such motors, methods of measuring energy efficiency, and the usage of energy-efficient motors with renewable energy sources. In the field of energy-efficient motor design and analysis, studies typically tackle topics such as material utilization, component geometry, and dimensions, as well as rotor and stator configuration. These researches are focusing on the designing new motors that offer greater efficiency and lower energy consumption. In industrial settings, energy efficient motors yield considerable energy savings. Research on energy efficiency measurement methods entails the study of measuring instruments, testing procedures, and standards. The objective is to ensure the use of the appropriate techniques for measuring and testing energy efficiency, thereby guaranteeing the accuracy and reliability of energy efficiency data. The research on energy efficiency of electrical machines is quite extensive and there is research in many areas. The overall aim of these studies is to decrease energy consumption, resulting in environmental benefits. IE4 efficiency refers to motors with high energy efficiency. The IE4 efficiency category represents the highest level of energy efficiency and mandates that motors attain an efficiency of over 94% at a minimum. Consequently, IE4 efficiency motors consume less energy than others, providing greater productivity at reduced costs. IE4 efficient electric motors are typically utilized in machines requiring high power for industrial applications. IE4 motors present significant energy savings, particularly in pump, fan and compressor applications. In addition, these motors are crucial for creating a sustainable environment as energy conservation reduces carbon dioxide emissions and diminishes environmental footprints. IE4 efficient motors may have a higher initial cost but offer significant energy savings in the long term, shortening the return-on-investment period. IE4 efficient motors is vital in terms of environmentally conscious practices.

2.2 STRUCTURE OF INDUCTION MOTOR

Induction motors comprise two main parts: the stator, which is stationary, and the rotor, which rotates. Both parts consist of silicon sheets that transmit magnetic flux. Induction motor rotors come in two types: squirrel-cage and slip-ring rotors . The rotor examined in this thesis is the squirrel-cage rotor, a commonly utilized component in general industry.

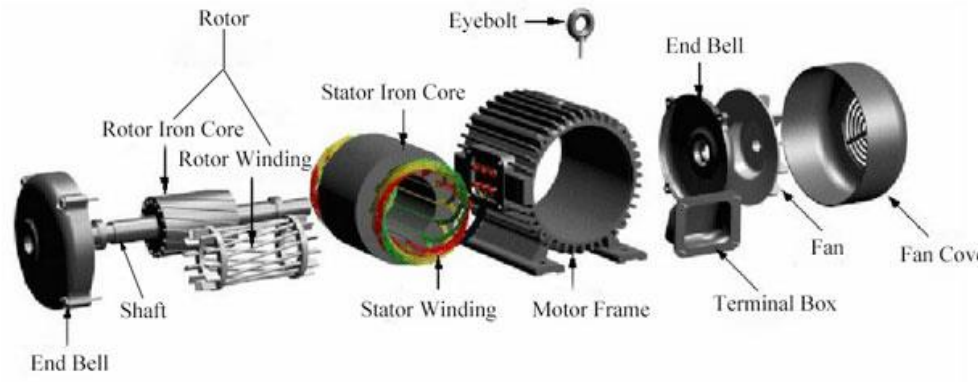

Figure 2.2: Parts of an Industrial Induction Motors

The efficiency, power factor, overload capacity, starting values, temperature rise, and magnetic noise of the induction motor are determined by the design of the stator and rotor windings. The active components of the motor are the sheet metal enclosures and windings. The motor's mechanical parts include the housing, shaft, bearings, end bells, cooling fan, and cooling fins.

2.2.1 Stator

The non-moving component of induction motors is referred to as the stator. It comprises two components, namely the stator core and the stator frame. The component which facilitates the stator windings and magnetic flux is known as the stator core. This core is assembled from an insulated lamination sheets, with one side being insulated to minimize losses from eddy currents. It is produced by compressing lamination sheets, each 0.5 mm thick, on top of each other. AC current-carrying stator windings are then placed in slots within the stator component. The windings can be wound in different winding types as one, two, three and multiphase. The stator frame houses both the stator core and windings. The stator frame enables the rotor to be supported on both sides while the motor is mounted on the stator body, offering the

option to connect it vertically or horizontally with the use of legs or flanges. The stator body is manufactured from either aluminum or cast iron. Additionally, the stator body features ducts positioned parallel to the motor axis, providing cooling for the motor [16, 17].

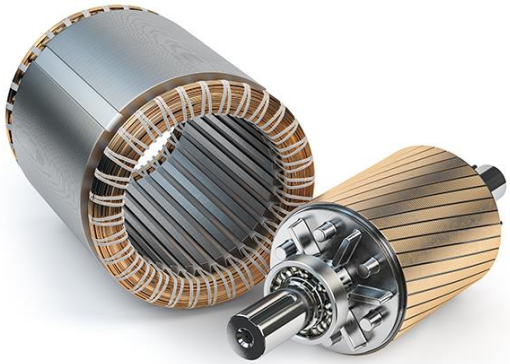

Figure 2.3: Stator and Rotor

The stator generates the magnetic field and houses the windings, which are supplied with alternating current. The use of alternating current results in the occurrence of hysteresis and eddy losses, which cannot be avoided. However, to mitigate these losses that impart heat to the iron structure, sheet materials with high induction and low hysteresis losses should be utilized for constructing the stator. These materials are specially cut and insulated by means of presses and moulds.

The sheets are electrically insulated to prevent the flow of eddy currents. They are then compressed in a press to form the stator sheet stack. The windings, prepared with the aid of special moulds, are placed inside the formed sheet stack. The resulting stator winding group is then pressed into the preheated body. The stator is fixed in place since it will expand after cooling down. The stator body structure is sealed using motor end bells. As the end bells hold the bearings to support them, a suitable surface is prepared for the rotor to turn on.

2.2.2 Rotor

The section of induction motors that rotate is called the rotor. It has two distinct parts: the rotor stack and the rotor winding. Much like the stator, the rotor stack stack is composed of compressed 0.35 mm - 0.5 mm thick siliconized sheets with one surface insulation. The winding is situated in slots within the rotor. The magnetic flux created

in the stator crosses the air gap and follows its magnetic field through the rotor stack. Furthermore, the rotor core functions as the component responsible for accommodating the rotor windings and transmitting the torque caused by the magnetic pathway to the shaft [17].

To mitigate the hysteresis and eddy losses induced by alternating current, a laminated stack is constructed within the rotor. To produce both rotor bars and rings, molten aluminium is injected into the rotor slots. Lastly, the outer diameter of the rotor is machined to the predetermined size, as per the calculated air gap.

The rotor windings are made with squirrel cage or three-phase windings and placed in slots. Induction motors are divided into two according to the structure of the rotor and rotor windings:

a) Squirrel cage (short circuit rotor) induction motors

b) Inductions motors with slip ring (wound rotor)

Squirrel Cage Induction Motors: These motors utilize copper or aluminum bars that are short-circuited with copper or aluminum rings at both ends and injection which are then placed in the rotor slots. Due to their resemblance to a squirrel cage, they are referred to as squirrel cage rotors. In small induction motors, the rotor winding is created by injection of aluminum into the rotor slots with specialist moulds [16].

Wound rotor induction motors feature slots in the rotor where three-phase star connected winding are placed. These winding leads are connected to the external circuit through the brush-ring structure on the shaft. By adding resistance or an independent voltage source to the rotor winding terminals, the speed and torque of the induction motor can be controlled [16].

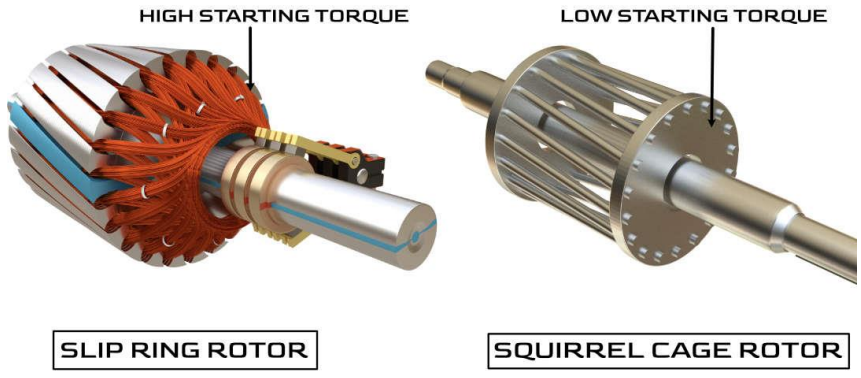

Figure 2.4: Slip Ring Rotor and Squirrel Cage Rotor

2.3 WORKING PRINCIPLE OF INDUCTION MOTOR

The operation of induction motors relies on the law of induction, requiring a time-varying magnetic field generated in the motor's air gap. Two methods for producing a variable magnetic field are possible: passing alternating current through stationary windings or moving the windings via direct current. To generate a magnetic field in the air gap of induction motors that fluctuates with time, alternating current is supplied to the fixed stator windings. The induction motor concept is based on the rules of rotating magnetic fields. There is a 120° phase shift between the electrically isolated magnetic fields located in the stator slots. When 3-phase windings are supplied from the mains, a voltage is induced in the stator windings and a current begins to flow. In accordance with Ampere's Law, a magnetic field is generated around the conductor in which current is flowing, resulting in a rotating magnetic field resulting from alternating current and voltage. Equations 2.1 and 2.2 provide details on Ampere's Law. The magnetic field rotates at synchronous speed and the magnetic field lines cut across the active material in the rotor slots. As per Faraday's Law, the bars induce voltage and current flows in the rotor bars due to their short circuit position in the cage with the end ring. Due to resistance, the rotor cage behaves like a load. Equations 2.3 and 2.4 describe Faraday's Law. According to Lenz's Law, the conductor through which current flows produces a counter magnetic field to counteract the magnetic field's effect that causes it, in the opposite direction. Lenz's law is presented in Equation 2.5.The rotor's magnetic field rotates continually as it attempts to catch that of the stator, but it can never attain synchronous speed, rendering it an 'induction machine'. If the rotor were to reach synchronous speed, induction would not occur, and there would be no current flow or torque generation.

In the formulae below, $\vec{H}$ represents the magnetic field strength in amperes per meter (A/m), $\vec{D}$ is the electric flux density in coulombs per square meter(c/m^2), $\vec{J}$ is the current strength in amperes per square meter A/m^2, and $d\vec{s}$ is the infinitesimal field element. $\vec{B}$ refers to the magnetic flux density measured in tesla (T), while ϕ_B is the magnetic flux (Wb).

$$\nabla.\vec{H} = \vec{J} + \frac{\partial \vec{D}}{\partial t} \tag{2.1}$$

$$\oint \vec{H} \,.\, d\vec{\ell} = \oint \vec{J}.\partial\vec{s} + \int \frac{\partial \vec{D}}{\partial t}.d\vec{s} \tag{2.2}$$

$$\nabla.\vec{E} = -\frac{\partial \vec{B}}{\partial t} \tag{2.3}$$

$$\oint \vec{E}.d\ell = -\int \frac{\partial \vec{B}}{\partial t}.\mathrm{d}\vec{\mathrm{s}} \tag{2.4}$$

$$\vec{E} = -\frac{\partial \phi_B}{\partial t} \tag{2.5}$$

2.3.1 Equivalent Circuit of an Induction Motor

The voltage induced on the rotor and the current flowing are due to the stator, similar to the transformer structure. Consequently, the induction motor equivalent circuit is comparable to the transformer circuit. The squirrel cage induction motor excites through the stator, and unlike synchronous machines, there is no excitation on the rotor side. As it is single-excited, two distinct voltages are not induced. From this perspective, a novel equivalent circuit method could be developed by examining the frequency and slip connections of the rotor through the transformer model [18]. If the magnetic fields of the rotor and stator begin to rotate at an identical speed, the voltage induced on the rotor will also reduce to zero. The amplitude and frequency of the induced voltage, which can be acquired between the minimum and maximum values, are determined by the rotor's slip [18].

The equation for slip in an induction motor is presented in section 2.6.

$$\%s = \frac{n_s - n_r}{n_s} \times 100 \tag{2.6}$$

In this equation, n_s represents the synchronous speed of the stator magnetic field $(min^{-1}).n_r$ is the speed at which the rotor rotates rated load (min^{-1}). The slip is expressed in percentage [18].

The synchronous speed of the motor is determined by equation 2.7, where f_s represents the stator frequency, p represents the number of poles.

$$n_s = \frac{120 \times f_s}{P} \tag{2.7}$$

If the speed of the rotor is the same as the synchronous speed, the slip is zero. If the rotor comes to a rotor speed zero then the slip will become one. The rotor speed can be determined by using the equations provided. Equation 2.8 gives the specific formula for the rotor speed.

$$n_r = (1 - s) \times n_s \tag{2.8}$$

Due to operational principles, the transformer equivalent circuit and the induction machine equivalent circuit display significant similarities. It is shown in Figure 2.5 shows the rotor equivalent circuit of the motor at any slip.

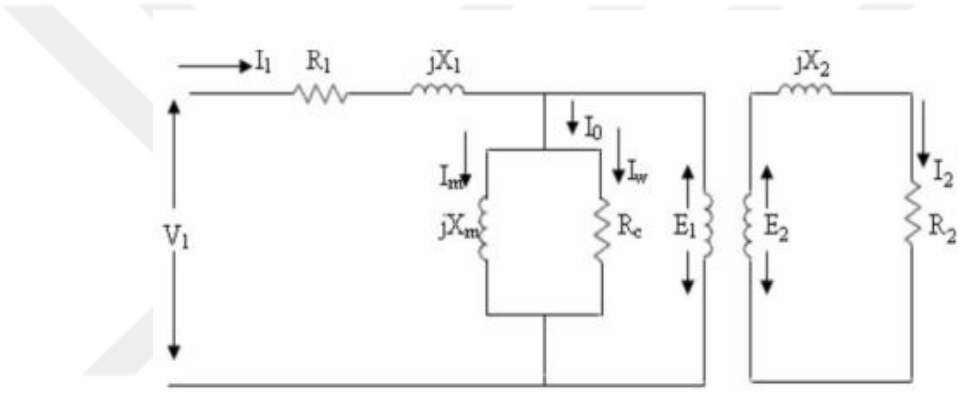

Figure 2.5: Representation of Transformer Circuit

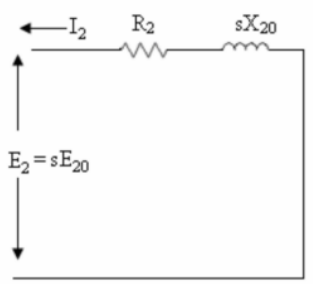

Figure 2.6: Rotor Equivalent Circuit (s Refers to Slip Value)

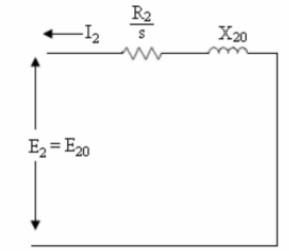

Figure 2.7: Rotor Equivalent Circuit (At Standstill)

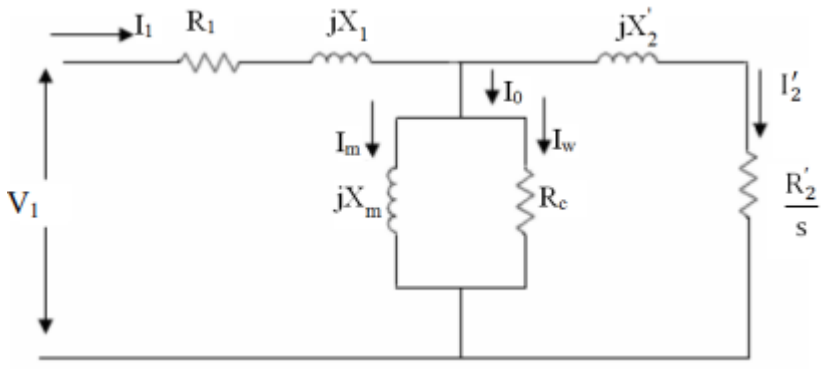

Figure 2.8: Equivalent Circuit of An Induction Motor Referred to Stator Side

Figure 2.8 shows the equivalent circuit of an induction motor referred to stator side.

2.4 LOSSES AND EFFICIENCY OF INDUCTION MOTOR

Motors perform the conversion of electromechanical energy.During the conversion process, electrical energy is supplied to the stator and passes through the stator windings, air gap, and rotor windings before ending at the shaft. Any difference between the input and output energies results in losses.

When 3-phase alternating current is applied to the stator windings of an induction motor with a short-circuited or wound rotor, a rotating magnetic field is created in the stator windings. This causes the rotor to rotate in the direction of the rotating field with a speed of n_r. If there is no load applied to the motor shaft, the rotation of the rotor closely matches that of the rotating field. The state in which the rotor is able to rotate without restriction is termed as the no load operation of the induction motor [20]. The no load motor test reveals frictional and iron losses experienced by the induction motor. The losses directly correspond to the power drawn from the network by the no load motor since the power captured from the motor's shaft is zero. A constant mechanical loss occurs only due to friction between the bearings and propellers with air. The 3-phase alternating current passing through the stator windings creates a rotating field that results in eddy and hysteresis losses, also known as iron losses in the stator core. During no load operation, since the rotating field speed cutting the rotor core is very low, the iron losses in the rotor are assumed to be zero. Moreover, because no current passes through the rotor short circuit bars, the rotor copper losses can be presumed to be zero as well. Phase currents through the stator windings results in heat losses due to the effective resistance of the copper windings.

Based on this information, the no load power of the induction motor is equal to the sum of stator iron, stator copper losses, and friction losses [20].

Losses in an induction machine are categorized as either no load or load. Abbreviations will be explained upon first use. No load losses comprise of iron and friction losses. Losses that occur during load consist of conduction losses in the stator and rotor windings, as well as additional losses due to the load. The technique for assessing electrical machine losses is specified by the International Electrotechnical Commission (IEC) in the IEC 60034-2-1 standard. To meet the efficiency levels outlined in the IEC 60034-30-1 standard published by IEC and earn IE (International Efficiency) classification, electric motors must undergo testing and have their efficiency calculated in accordance with the IEC 60034-2-1 standard.

To determine the losses, the motor undergoes the tests outlined in the standard procedures. The first of these is the rated load test. Before commencing this test, the temperatures of the winding and the ambient environment are measured. The motor is loaded at the rated load and operated until it achieves the thermal equilibrium state. It is subsequently operated under rated load until there is no alteration of 1 °K or 1 °C in the windings within a duration of half an hour.

When there is no 1°C change in temperature of half hour, we measure the input power, motor torque value, average line current, phase-to-phase voltage, rated speed, winding temperature, phase-to-phase stator winding resistance, and stator winding phase resistance.

At rated load there are stator copper losses and rotor losses. $Pcus$ represents stator copper losses, I represent line current, R represents phase-to-phase resistance. Values for star and delta connections are shown in Equation 2.9,2.10,2.11.

$$P_{cus} = \frac{3}{2} I^2 . R \tag{2.9}$$

$$P_{cus} = \frac{3}{2} I^2 . 2R_1 \tag{2.10}$$

$$P_{cus} = \frac{3}{2} \left(\sqrt{3} I\right)^2 . 2R_1 \tag{2.11}$$

Copper losses in the rotor (P_{cur}) can be determined by multiplying the slip value (s) while subtracting the stator's copper and iron losses (P_{fe}) from the input power. Values are shown in Equation 2.12.

$$P_{cur} = \left(P_1 - P_{cus} - P_{fe}\right).s \tag{2.12}$$

After completing the rated load test, the load curve test commences. After loading the motor at 1.25, 1.15, 1.0, 0.75, 0.50 and 0.25 times, the recorded values are used to calculate the stator and rotor losses at each point.

The no-load test is carried out after completion of the nominal load and load curve tests. The ratio of the voltage value to the rated voltage is used to calculate the iron and friction losses. Resistance is measured both before and after commencing the test. The voltage to rated voltage ratio is 1.10; 1.00; 0.95; 0.90; 0.90; 0.60; 0.50; 0.40 and 0.30. The initial four ratios denote iron losses, while the last four ratios denote friction losses.

To determine the constant losses, subtract the stator winding losses in the no-load running experiment from the input power. Alternatively, the losses can be calculated as the sum of wind, friction, and iron losses. Technical abbreviation definitions will be provided upon initial use.

Iron Losses

Surface losses

Pulsation losses

Transmission losses

Additional losses

Air and bearing friction losses

Induction motors have various losses associated with them, which can be categorized as either core or mechanical losses [22]. Core losses occur in both the stator and rotor cores and are dependent on the supply frequency and flux density [22]. These losses are hysteresis and eddy current losses, while the stator iron core has a practically constant loss and the rotor iron core has a negligible loss [22]. Rotor core losses are high at the start and during acceleration, and the sum of friction, windage and core losses are almost constant throughout the speed range [23]. Friction and windage losses, which are also known as rotational losses, are zero at the start and

increase as the speed increases [23]. Additionally, copper losses occur in the stator and rotor windings and are dependent on the current in the windings; these are also known as electrical or I^2R losses [22]. Stray load losses are all losses not covered by the other types of losses, and harmonic fields can also cause losses in induction motors [23]. All of these losses cause a decrease in motor performance, and they can also cause heat and noise problems [24]. Therefore, it is important to understand the sources and types of losses in electric motors [24] in order to minimize their effects and increase motor performance.

Induction motor losses can be divided into three main categories; copper losses, iron losses, and friction and windage losses [22]. Copper losses occur in both the stator and rotor windings due to winding resistance [25], and iron losses also take place in the stator and rotor cores. Friction and windage losses occur in the bearings of the motor and due to the rotor spinning [26]. In addition to these types of losses, there are also constant and variable losses. Constant losses include the stator core losses and mechanical losses, while variable losses are the stator copper losses and rotor copper losses [27]. All of these losses can have a major negative effect on the efficiency of the motor, meaning that steps must be taken in order to minimize them. The power flow diagram of an induction motor outlines the input given to the motor, the losses occurring, and the output of the motor [23]. This diagram can be used to identify the areas where losses are most significant, allowing for a more effective way to reduce them [24]. This can be achieved by improving the cooling system, using better materials, and altering the design of the motor. Reducing the core losses in induction motors can lead to several advantages such as improving motor efficiency and reducing energy waste [24]. Ultimately, the aim should be to minimize the losses in induction motors in order to improve performance and maximize efficiency [28].

All these losses decrease the efficiency of the induction motor [27]. Induction motors also have a high ohmic loss in the rotor, which makes it difficult to remove the heat from the rotor [26]. Due to this, the induction motor needs more input power to achieve the desired output [27]. The power flow diagram of induction motor is a pictorial representation of the input given to the motor, the losses occurring and the output of the motor [23]. This diagram shows that the output of the motor is always less than the input given to the motor [23]. It also helps to identify the components of the induction motor which are responsible for the losses, leading to increased efficiency of the motor [23].

There are several techniques available to minimize these losses, which need to be reduced in order to enhance productivity. Eddy current losses, which are a form of iron loss, are dependent on sheet thickness. To minimize these losses, the sheet thicknesses used in the stator and rotor can be reduced. Hysteresis losses, also an iron loss, can be reduced by using first-class sheet metal of higher quality. Copper is a more conductive material than aluminum and its use on the rotor side can reduce copper losses. Expanding the size of the motor results in a decrease of flux density inside the iron components, reducing the density of current within the windings. As a result, losses from iron and copper are diminished. Enlarging the dimensions of the motor also improves the heat dispensation. Modifying the designs of the stator and rotor slots present another significant choice in loss reduction. A fan with superior design, levelling reduced friction and upgraded airflow, is another method to reduce friction and ventilation losses [29].

The use of centrifugal rotor casting for the aluminum squirrel cage, instead of common high- and low-pressure casting, boosts the conductivity of the rotor bars and rings while decreasing rotor copper losses. The cutters employed in laminating printing moulds must be as sharp as possible to prevent lamination short-circuits. It is crucial to avoid core and winding scratches during transport [30].

To mitigate core losses, one can utilize various methods such as extending the stack length, augmenting the outer diameter, implementing heat treatment, and employing low-loss steel sheet. Increasing the stack length is a simpler approach to tackle this issue. Optimizing the length of the stack will enhance efficiency. Enhancing the stack length has the same effect as increasing its outer diameter, but the costly moulds serve as a drawback. By applying heat treatment to the stator and rotor cores, magnetic and energetic characteristics of these components can be transformed, thus reducing hysteresis losses. It is possible to decrease eddy currents and iron losses by thinner laminated sheets [29].

Nonetheless, such an action will come at increased cost as more sheet metal will be necessary to achieve the desired stack size [30].

By utilizing amorphous steel, eddy currents are reduced as it is thinner than standard laminations.

The loss coefficients employed in the hysteresis losses of low loss steel sheets are low. Nonetheless, the magnetization curves of these sheets exhibit dissimilarities [30].

It is possible to minimize mechanical losses in bearings on the shaft and in motor covers. To reduce bearing losses, oil with a low coefficient of friction should be used. Additionally, the design of balls inside the bearing should be enhanced. In the tests carried out with bearings with increased efficiency, friction losses were reduced and improvement was achieved depending on the motor [31].

Effective cooling can be achieved through fan design. Specifically, reducing the diameter of the fan and improving the cooling process will lead to a decrease in fan losses.

To minimize stator losses, it is essential to enhance the slot fill factor, ensure effective winding and wire insulation, and decrease the winding lead length. Reducing both current density and copper losses is possible with high slot fill factors, due to the change in wire diameter and the reduction in resistance.

Variation in wire diameter has an impact on the reduction of resistance and current density as well as copper losses. Higher slot fill factors can contribute to these effects. Technical abbreviations will be explained when first referred to.

When using round wires, the stator slot fill factor ranges from 0.65 to 0.75, taking into account the insulation on the wire wall [31].

Winding head lengths (end windings) protruding from the stator lamination cause both copper losses and leakage flux. Therefore, by reducing the winding head lengths, copper losses can be minimized, and the reduction of leakage fluxes can be achieved [31].

Insulation with higher thermal conductivity can increase winding temperature, resulting in better cooling of the motor and lowered winding losses due to reduced winding resistance. This can lead to achieving higher power densities [31].

CHAPTER III
EFFICIENCY CLASSES, REGULATIONS AND DESIGN CRITERIA

Induction motors are widely used in various industrial and commercial applications due to their simple design and robust construction. As the demand for energy-efficient technologies increases, there has been a growing focus on improving the efficiency of induction motors. It will then examine the regulations that have been put in place to ensure that induction motors meet the required energy efficiency standards.

In Turkey, induction motors consume 90% of the electrical energy utilized by electric motors. Induction motors are responsible for approximately 30% of the country's total national electricity consumption and 70% of its industrial electricity consumption [32].

The International Electrotechnical Commission (IEC) has established a set of global standards for energy efficiency in electric motors [32]. This international standard IEC 60034-30-1 defines efficiency classes for low-voltage three-phase AC squirrel cage motors [21]. The efficiency classes are identified by the letters IE, which stands for International Efficiency, and are denoted by a code in accordance with the international standard IEC 60034 Part [21, 31, 33]. The idea of defining efficiency classes for electric motors was initially proposed by the manufacturers on a voluntary basis, however, the increasing demand for energy-efficient drives and the need for a uniform standard for energy efficiency led to different regulations for determining motor efficiency [33]. The new standard IEC 60034-30-1 defines four energy efficiency classes or IE efficiency classes: IE2, IE3 Premium, IE4 Super Premium, and IE5 Ultra-Premium [33]. IE2 is an efficiency class for induction motors, and is mandatory for motors with rated output greater than 0.12 kW [33]. Furthermore, IE2 efficiency class applies to versions with 2, 4, 6 or 8 poles, and to uncooled TEAO versions [33]. IE3 Premium efficiency class is mandatory for electric motors with a rated output between 0.75 kW and 1000 kW while the IE4 Super Premium efficiency class applies to electric motors with rated outputs between 75 kW and 200 kW with 2,

4, or 6 poles [33]. The new measurement procedure determines additional losses more precisely than previous methods, and motors identified with the new IE code must be measured according to the new measurement procedure according to IEC 60034-2-1:2014 [33]. The designation for the efficiency classes is based on the designation for IP protection classes [33], and the standard applies to applications in ATEX environments [33]. The efficiency classes of induction motors are globally standardized, providing an international platform for comparison of motors and facilitating international trade [33]. Manufacturers, such as MENZEL Elektromotoren, have to adhere to the IEC standards for energy efficiency. The IEC 60034-1 provides the regulatory framework for the type plate of low-voltage three-phase squirrel cage motors [33]. This standard also enables international comparison and certification of electric motors [33]. The IEC 60034-1 specifies the labeling requirements for energy efficiency classes of three-phase squirrel cage induction motors [33]. This standard facilitates the switch from EFF code to the uniform IE code, thereby enabling international comparison of motors in terms of energy efficiency [33]. Additionally, the standard IEC 60034-1 aims to standardize regulations globally [33]. This ensures that all induction motors meet the same standard to ensure their energy efficiency [33]. As a result, the standard IEC 60034-1 offers a uniform global basis for the assessment of individual low-voltage induction motors [33]. MENZEL Elektromotoren provides information relating to the efficiency of induction motors, though their type plate does not provide any data on how this efficiency affects their overall performance [32]. The nameplate of the motors is standardized by the IEC 60034-1, which requires the energy efficiency class and efficiency level to be stated [21]. Furthermore, the standard also allows motors designed for different operating modes to be operated permanently with rated output. This means that the motors need to be designed to operate at their specified efficiency for its rated output [32]. Therefore, the efficiency of the induction motors can affect the performance of the motor in terms of its output and power consumption [32]. As the efficiency of the motor increases, so does its output and power consumption. This means that the motor can produce more power with less energy, thus reducing the overall cost of operation. Additionally, improved efficiency can help reduce the environmental impact of the motor, as less energy is needed to produce the same output [32]. This is also beneficial for cost savings, as it reduces the amount of energy consumed, which can help to reduce the overall cost of operation.

The International Electrotechnical Commission (IEC) has established a set of global standards for energy efficiency in electric motors, which includes four energy efficiency classes: IE2, IE3 Premium, IE4 Super Premium, and IE5 Ultra-Premium. The new standard IEC 60034-30-1 defines these classes and their specific requirements. The aim of these regulations is to standardize efficiency standards globally, which is crucial given the increasing demand for energy-efficient drives and the need for a uniform standard for energy efficiency. The labeling requirements for energy efficiency classes of three-phase squirrel cage induction motors are specified in the IEC 60034-1. Future research could focus on a more in-depth analysis of the effectiveness of these regulations and their impact on reducing energy consumption.

It was established in November 2008 by the International Electrotechnical Commission for induction motors as IEC 60034-30:2008 to serve as an international efficiency standard across all countries to achieve universal standardization. The IE Standards were released by the European Community (EU) in July 2009 through regulation 640/2009, which was developed from the IEC 60034-30 standard. As of November 2010, the measurement of motor efficiency under IEC 60034-2:1996 is no longer applicable and has been replaced by IEC 60034-2-1:2014. IE efficiency standards have been legally enforced in the European Community for all 2, 4 and 6 pole induction motors with frequencies of 50/60 Hz and voltage up to 1000 V, ranging from 0.75 to 375 kW since 16.06.2011.

In 2008, the IEC extended the legal regulation on energy efficiency for motors within the power range of 0.75 kW to 375 kW, introducing new definitions for efficiency classes. Efficiency classes are now organized based on frequency, power, and number of poles, as outlined below in the IEC 60034-30 standard [21].

IE4 Super Premium Efficient Motors

IE3 Premium Efficient Motors

IE2 High Efficiency Motors

IE1 Standard Efficiency Motors

In compliance with the efficiency classifications outlined in the IEC 60034-30:2008 standard, the acquisition and utilization of IE2 efficiency class motors in the United States were authorized between 1998 and 2011, followed by a transition to IE3 efficiency class motors from 2011 onwards [21].

In both the EU and China, the use of IE2 efficiency class motors became mandatory from 2011 to 2015, and IE3 efficiency class motors were made compulsory

after 2015. Meanwhile, in Turkey, the shift to IE2 efficiency class became mandatory in 2012, IE3 became compulsory in 2015, and IE2 motors are exclusively authorized for use with a variable frequency drive [35].

Other countries have implemented regulations to align with IEC/NEMA standards. During this period, the provisions outlined in EU Regulation 2019/1781, incorporating the notion of "Eco-design" for electric motors, have been implemented [36].

IE1 (Standard Efficiency): This class denotes the minimum efficiency level mandated by the IEC standard. Motors in this class are typically older and less efficient designs.

IE2 (High Efficiency): Motors in this category have superior energy efficiency compared to IE1 motors and are designed to be more energy efficient. This category is generally associated with motors of better efficiency.

IE3 (Premium Efficiency): Motors in this category offer even greater efficiency than IE2 motors and are widely acknowledged as being highly energy efficient. Many regulations around the globe require the use of IE3 motors in specific applications.

IE4 (Super Premium Efficiency) is the topmost efficiency category according to the IEC standard. Motors belonging to this category are engineered to deliver exceptional energy efficiency and are employed in situations where minimizing energy consumption is of utmost importance.

Specific regulations and requirements for motor efficiency can differ depending on the country and region. Numerous countries and regions have established their individual standards and regulations for enhancing energy efficiency in electric motors. These are frequently based on or aligned with international standards, such as those of the IEC.

In the European Union, for instance, EC Regulation 640/2009 provides an overview of motor efficiency regulations. In the United Kingdom, the Department for Business, Energy & Industrial Strategy (BEIS) establishes energy efficiency criteria for electric motors.

It is crucial to take into account the relevant regulations in your location and opt for motors that meet the required efficiency class to encourage energy conservation and ecological sustainability when choosing electric motors.

Recently introduced regulations are in line with the industry that uses induction motors in its products. Despite the increasing use of high efficiency (IE4) induction motors, their design and usage remain challenging.

3.1 DESIGN CRITERIA OF INDUCTION MOTOR

3.1.1 Design of Electric Motors

The design of electrical machines includes critical components for improving energy efficiency. The design of the stator and rotor is crucial for achieving optimal energy efficiency in electric machines. Careful consideration of both design and material selection is essential for maximizing energy efficiency. Therefore, meticulous attention to the stator and rotor design is necessary for achieving the best possible energy efficiency in electric motors. The stator is the stationary component responsible for generating the magnetic field, while the rotor is the rotating part that moves under the influence of the magnetic field. The design of the stator and rotor is crucial for achieving optimal energy efficiency in electric machines.

3.1.1.1 Design Criteria of Stator

The stator's design holds a particularly important role in producing the magnetic field. Homogeneous magnetic flux distribution and a strong magnetic field enhance motor efficiency. To achieve this, factors such as the magnetic flux density of the stator, magnetic field uniformity, energy loss, and temperature rise require consideration. The selection of stator material is also crucial for efficiency. Typically, laminated silicon steel is used in stators, whilst amorphous materials feature in new generation high efficiency motors. Efficient motor performance depends on rotor design. Factors such as the rotor's magnetic field generation, magnetic flux density, rotor temperature, and energy losses significantly impact the motor's efficiency. Increasing the rotor's magnetic flux density necessitates the consideration of factors including the utilization of magnetic materials and the geometry of the rotor surface. Rotor materials made with magnetized materials having high magnetic flux permeability or high conductivity alloys are frequently used. In high-efficiency motors, magnets with a high magnetizing field and aluminum rotors are utilized.

Thus, the design of the stator and rotor is very important for the energy efficiency of electric machines. Several significant factors, such as magnetic flux density, uniformity of the magnetic field, rotor material, and geometry, affect the

motor's efficiency. Innovative designs, including amorphous materials, magnets with a high magnetic field, and aluminum rotors, are utilized in high-efficiency motors.

The precise geometric dimensioning of the stator is of paramount importance for achieving optimal energy efficiency in electrical machines. The stator's dimensions directly impact the strength, intensity and distribution of the magnetic field - all of which significantly influence the motor's performance and energy efficiency.

The stator's geometric dimensions are determined by a range of factors, including the number of stator slots, their shape, width, depth, diameter and angle. Each of these factors is essential to the generation and distribution of the magnetic field.

The number of stator slots impacts this distribution. A lower number of slots results in higher magnetic flux at lower frequencies, whereas a higher number produces lower magnetic flux at higher frequencies. Furthermore, slot shape also plays a role. Trapezoidal and rectangular shapes are the most typical slot shapes affecting the distribution of the magnetic flux. The width and depth of the slots impact the magnetic flux density of the motor. Broader and deeper slots permit greater magnetic flux density, whereas shallower and narrower slots may lead to reduced magnetic flux density.

The diameter of the stator governs the strength of the magnetic field. A bigger stator diameter results in a stronger magnetic field, while a smaller stator diameter leads to a weaker magnetic field. The slot angle impacts the uniform distribution of the magnetic field on the stator's surface.

The size of the stator is directly related to the generation and distribution of the magnetic field and impacts the performance and energy efficiency of the motor. Therefore, geometrical sizing plays a crucial role in the motor's functioning and must be optimized accordingly. The number of stator slots, slot shape, width, depth, stator diameter and angle are all factors that affect properties including magnetic flux density, strength, and uniformity of the magnetic field.

The geometric dimensioning of the rotor plays a vital role in determining the energy efficiency of electrical machines. It affects the magnetic flux density, strength, and distribution, thereby impacting the performance and energy efficiency of the motor.

3.1.1.2 Design Criteria of Rotor

Induction motors are widely used in various industrial applications due to their rugged construction, simple design, and low maintenance requirements. However, the efficiency of these motors has become a critical issue in recent years, and there is a growing demand for high-efficiency motors to reduce energy consumption and operating costs. In response to this demand, the International Electrotechnical Commission (IEC) has introduced standards for induction motors with a minimum efficiency level of IE4.

Design of an IE4 efficiency class induction motor requires careful consideration of certain criteria. One of the most important aspects is choosing the appropriate slot combination [46]. This is because selecting an unsuccessful combination can result in parasitic torque, vibration and noise. As recommended by the NEMA standard, there are four rotor bar shapes available for induction motors, with Class D being the most suitable for designing Low Speed Permanent Magnet Synchronous Motors (LSPMSM) [46]. Furthermore, it is important to determine the outer diameter of the stator and rotor, which can be calculated using the sizing method [45]. In addition, the shape of the rotor aluminum bar should be determined based on the NEMA class [45]. To find the optimal design, Finite Element Analysis (FEA) and Design of Experiments (DOE) can be employed to maintain the outermost size of the induction motor [46]. Once the design has been finalized, its performance should be verified through an experiment to ensure that the desired efficiency has been achieved [46]. Additionally, it is necessary to use rare earth magnets (neodymium) as the permanent magnet of the LSPMSM, and advanced die-casting technology is not needed for manufacturing IE4 class induction motors with LSPMSM [45]. Finally, increasing the diameter of rotor bars can reduce the resistance of the rotor bar, shorten the settling time for steady-state, and increase the starting torque of the motor [46]. Efficiency improvement measures for induction motors involve design techniques to reduce losses and increase efficiency [47]. To get IE4 efficiency, several techniques have been proposed such as increasing the stator core length, skewing of rotor bars and rotor slot insulation [48]. The main design change to reach the IE4 efficiency class consists of a significant increase in the stator slot fill factor [49]. Many manufacturers have achieved the IE3 and IE4 classes by redesigning the entire motor series, with a combination of harmonic winding and rotor slot painting [50]. To reach the IE4 efficiency class, a copper rotor is one of the best options [51]. Recently, a design of a

high-efficiency induction motor prototype of an induction motor has been introduced [52]. This design is capable of reaching IE4 efficiency levels by using die cast rotors, optimization of core length, winding and rotor shape [53]. In addition, a synchronous reluctance machine (PMASynRM) with a cage rotor has been proposed to achieve IE4 efficiency level [54]. The results show that SynRM can achieve IE4 efficiency level, confirming that such an approach can be used to obtain IE4 efficiency in induction motors. Thus, a combination of various design techniques can be used to push IE3 motors towards the IE4 class.

3.1.2 Stator, Rotor Windings and Resistance

Electric motors, especially those employed in propulsion systems, depend on several motor parameters such as armature/rotor and stator resistance to operate effectively [37]. Among these parameters, rotor resistance is a crucial consideration for induction motors. Any variation in rotor resistance may lead to performance degradation and cause significant changes in the model of induction motors [39]. A common approach to mitigate the effects of stator resistance on motor performance is to assume accurate motor inductances [40]. However, when rotor resistance is not accurately estimated, power efficiency and performance of the motor degrade, leading to various issues such as noise, voltage distortion, and inaccuracies in modeling [41]. Current research focuses on developing new concepts of stator resistance that incorporate mechanical losses effects. An observer with online rotor/stator resistance estimation has been proposed for induction motors with one phase current [42]. To examine the effects of stator resistance and variation on motor performance, researchers have studied the performance of stator and rotor resistance estimators and torque and flux responses of the drive [43]. Furthermore, the parametric study has been conducted to analyze the effect of stator and rotor slot dimensions on different performance aspects, including the effective rotor resistance, which is influenced by skin effect [44]. The transient performance of the rotor resistance estimator is critical in ensuring optimal motor performance. The line-tuned stator resistance and rotor resistance estimate track can minimize the distortion effect introduced by rotor resistance [45].

3.2 OPTIMIZATION STEPS OF INDUCTION MOTOR

The design of induction motors requires optimization studies to be carried out on motors with the following parameters;

- Different stator/rotor slots combinations will be explored in this study.
- The optimization of stator/rotor slots will also be investigated.
- Studies will be conducted to optimize the air gap length.
- The selection of appropriate core materials will be determined.
- The determination of stator winding type (e.g. distributed winding, concentrated winding, hairpin) will be made.
- Specific electrical and magnetic loading values will be determined, which are important for sizing studies.
- The identification of performance parameters (yield, cost, weight, etc.) to be optimized.
- Identification of insulation materials to be used in the motor, with regards to their thermal load on the motor.
- Ongoing activities to determine the number of motor poles based on the number of Stator/Rotor slots combinations.
- Below are the design criteria required to translate the needs into design inputs.
- Efficiency: The design will aim for optimum performance by achieving high efficiency across a wide torque-speed range to ensure overall total efficiency during operation.
- Frame Characteristics: A body design that can successfully withstand the shock and vibration tests specified in the IEC 61373 standard will be developed.
- A motor with a power output of 110kW, commonly used within the industry and by customers, will be designed.
- The rated speed of both motors to be designed will be 1500 rpm, with a rated voltage of 380 V.
- Motor Cooling Specification: The cooling type will also be specified. The motor will feature a TEFC.
- Housing Material: Cast iron material with high strength will be used in housing and cover materials.

- Core material will be M400-50A silica sheet.

Once the model has been outlined, the next step will be optimization, which is depicted in the following diagram.

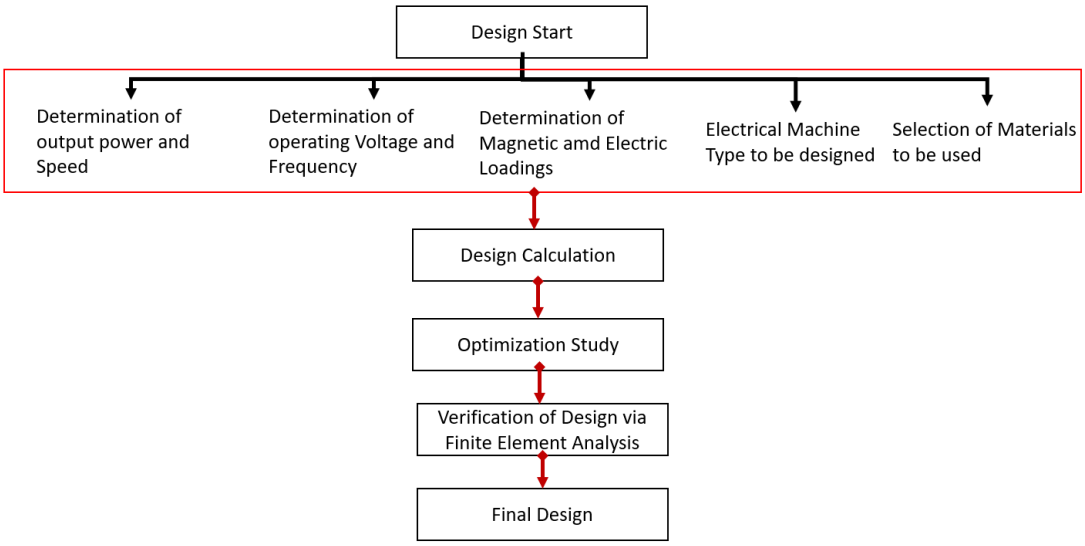

Figure 3.1: Design Steps for Induction Motors

Before commencing the design calculations, it is important to obtain fundamental information about the electric machine. It is essential to analyze Figure 3.1 as part of this process. This includes the output power and speed, which can be determined before the design. Alternatively, the designer must estimate certain parameters such as magnetic and electrical loads.

Once all necessary parameters are acquired, design calculations can be carried out. Due to the intricate nature of designing electrical machines, an initial basic model is obtained before optimization. To verify this optimized model, known as the design, finite element analysis is utilized, ultimately completing the process.

The design of electrical machines starts with dimensioning calculations and multiple parameters need to be estimated at the beginning.

- Rated Speed
- Rated Power
- Rated Type
- Cooling Method of the Machine
- Rated Voltage
- Phase Number of the Machine

- Machine Operation Regime [S1-S9]
- Desired efficiency as a result of design
- Economic and manufacturing limitations
- The International Electrotechnical Commission (IEC) investigates eight different types of working regimes, namely
- S1 - Continuous Operation,
- S2 - Short-Term Working,
- S3 - Intermittent Periodic Operation,
- S4 - Intermittent Periodic Operation with Departure,
- S5 - Intermittent Periodic Operation with Electric Braking,
- S6 - Continuous Operation with Intermittent Load,
- S7 - Continuous Operation with Electric Braking,
- S8 - Continuous Operation with Periodic Changes in Load and Speed.

During continuous operation, the motor operates at a constant load for a sufficient amount of time to reach the equilibrium temperature. This is the most commonly used type of operation, and the design in this thesis is based on continuous operation. In short-term operation, the motor cannot operate for long enough to reach equilibrium temperature, although the stopping times are sufficient for the motor to return to ambient temperature. In intermittent periodic operation, thermal equilibrium is never achieved due to consecutive and identical start and stop periods with constant load. An example of this is a motor involved in drilling or capping in a mass production line. Excess current drawn during start-up operations increases temperature. During electric braking, heat rise occurs in addition to take-off. Continuous operation with intermittent load exhibits similar heating patterns as periodic operation, but the temperature fluctuations occur due to the varying load instead of motor stopping, and there is no pause in operation. In contrast, continuous operation with electric braking depicts a graph akin to that of intermittent load operation, but in this case, the heat changes are a result of braking. In continuous operation with periodic changes in load and speed, there are observed periodic fluctuations in temperature due to changes in both induction motor speed and load. The graphs displaying lost power for these operating classes are shown below. It is crucial to consider these powers, which manifest as heat, when selecting the induction motor power. The determination of induction motor power requires careful consideration of operating regimes. The

selection of a lower power for the motor is possible depending on the load it operates with. The motor is required to reach thermal equilibrium with its surroundings, which is crucial during periods like rotation, low load operation, or cooling until it reaches ambient temperature. These factors enable the motor to function within the S1 operating regime for various types of operation. Failure to do so may have an impact on the motor's performance.

CHAPTER IV
MODELLING OF THE REFERENCE MOTOR

This chapter describes the examination of a reference motor using ANSYS Maxwell, a simulation tool for designing electric motors. The motor will be designed and analyzed in the simulation program, and then tested in the laboratory to establish the design and test ratio. The thesis describes the use of a reference motor to improve the design and increase design realism, leading to more accurate test results. The cost of the reference motor is taken into consideration to reduce costs in the new design. The thesis also mentions a detailed examination that was conducted to extract motor information.

In the thesis, a 48-36 slot motor model was chosen as a reference. The motor has 48 stator slots and 36 rotor slots. The number of slots and geometries for the motors to be prototyped will become clear once the design optimization studies are finished.

A reference study was carried out initially to determine the deviation between the simulation studies to be conducted within the project's purview and the test. For this study, a general purpose industrial motor of the EMTAŞ brand was disassembled, examined, and modelled for simulation. It has been observed that the studied motor is a classical induction motor with an aluminum rotor conductor and a distributed winding structure in the stator, similar to that of industrial induction motors. While the stator and rotor structure of the motor to be developed within the scope of the thesis is different, it is deemed appropriate to conduct a comparative study with this motor to determine the design-to-test ratio. Finite element analyses of the EMTAŞ brand induction motor, whose design was verified as a result of analytical analyses, were performed.

In order to shorten the duration of the transient finite element analyses to be performed in the Ansys Maxwell program, the analyses of the ¼ model were performed thanks to the symmetrical geometry of the motor. While this does not change the analysis results, the analysis time is reduced by ¼.

Table 4.1: Data of Reference Motor

Design Parameter	Value
Stator outer diameter (mm)	500
Stator inner diameter (mm)	330
Rotor outer diameter (mm)	327.350
Rotor inner diameter (mm)	115
Motor length (mm)	250
Number of stator slots	48
Number of Rotor Slots	36
Pole	4
Phase number (m)	3

Table 4.2: Dimensions of Stator Slot of Reference Motor

Stator Slot Geometric	Design
Hs0 [mm]	0.71
Hs1 [mm]	-
Hs2 [mm]	34.4
Bs0 [mm]	4.2
Bs1 [mm]	14.6
Bs2 [mm]	25.9
Rs [mm]	0

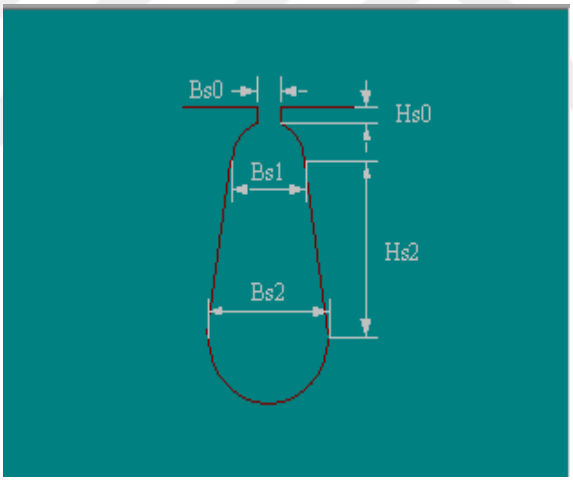

Figure 4.1: Demonstration of Dimensions of Stator Slot

Table 4.3: Dimensions of Rotor Slot of Reference Motor

Rotor Slot Geometric	Design
Hs0 [mm]	0.1
Hs01 [mm]	0
Hs2 [mm]	0.01
Bs0 [mm]	0
Bs1 [mm]	7.5
Bs2 [mm]	7.5

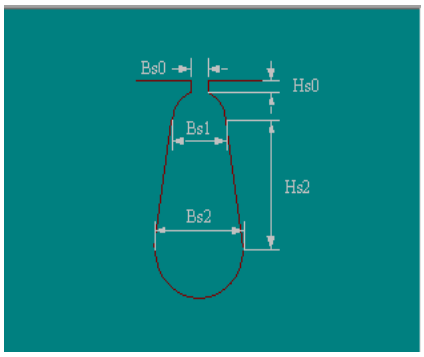

Figure 4.2: Demonstration of Dimensions of Rotor Slot

Table 4.4: Dimensions of Rotor Bottom Slot of Reference Motor

Rotor Bottom Slot Geometric	Design
Hs0 [mm]	4.8
Hs2 [mm]	32.55
Bs0 [mm]	2.4
Bs1 [mm]	10.8
Bs2 [mm]	5.2

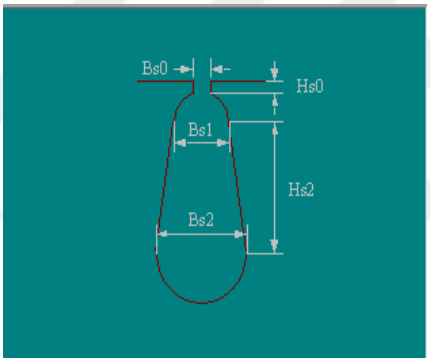

Figure 4.3: Demonstration of Dimensions of Rotor Bottom Slot

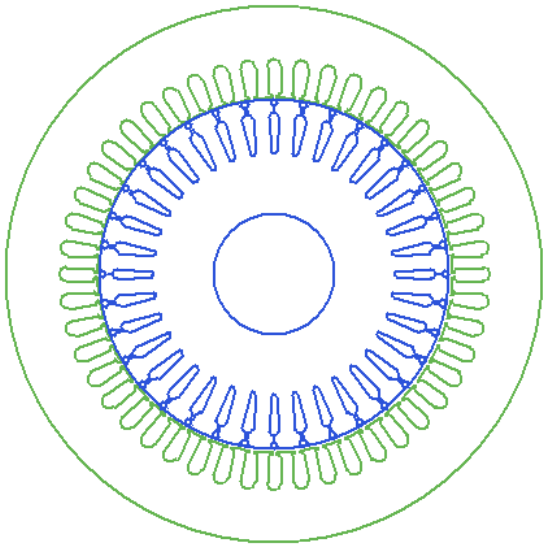

Figure 4.4: Design of Reference Motor in RMXPRT

Even though the stator and rotor design of the motor being developed within the thesis is different, it is deemed suitable to conduct a comparative study with this motor to ascertain the design/test ratio Table 4.5 presents the geometrical properties of the reference motor.

Table 4.5: Reference Motor Geometrical Properties

Design Parameters	Value
Stator outer diameter (mm)	500
Stator inner diameter (mm)	330
Rotor outer diameter (mm)	327.350
Rotor inner diameter (mm)	115
Motor length (mm)	250
Number of stator slot	48
Number of rotor slot	36
Pole	4
Phase Number (m)	3

Finite element analyses of the EMTAŞ brand induction motor, whose design was verified as a result of analytical analyses, were performed.

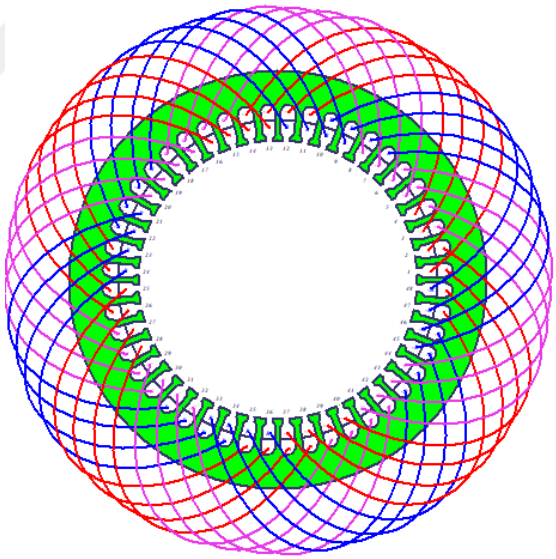

Figure 4.5: Representation of Reference Motor's Coil Windings

Table 4.6: Reference Motor's Coil Windings Data

Parameter	Value
Winding Layer	2
Winding Type	Whole-Coiled
Parallel Branches	4
Conductor Per Slot	26
Number of Strands	6
Wire Size	1.30 mm

The stator and rotor laminations of the motor under consideration are made of M530-50A silicon sheet. Cooling is achieved through the use of an aluminum propeller. The stator winding has copper windings, and the rotor rods are made of aluminum casting. A motor model will be created and tested analytically using an analysis program before conducting finite element analysis. The outcomes obtained through the established model will be presented alongside the test outcomes of the sample fabricated within laboratory surroundings, in compliance with the standards. Subsequently, we will disseminate the findings derived from the finite element method analysis and accompanying graphs.

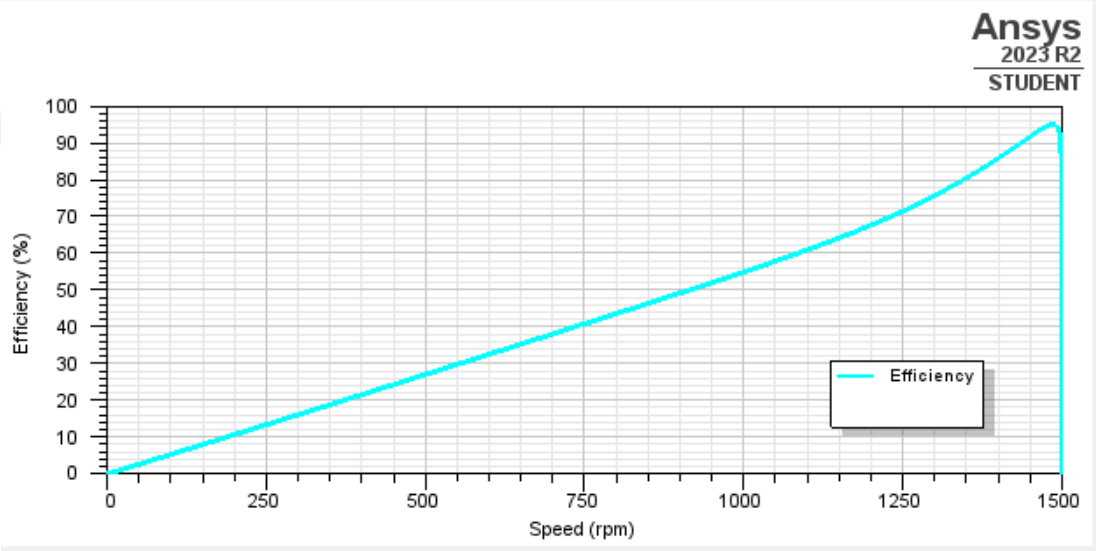

Figure 4.6: Efficiency – Speed Curve

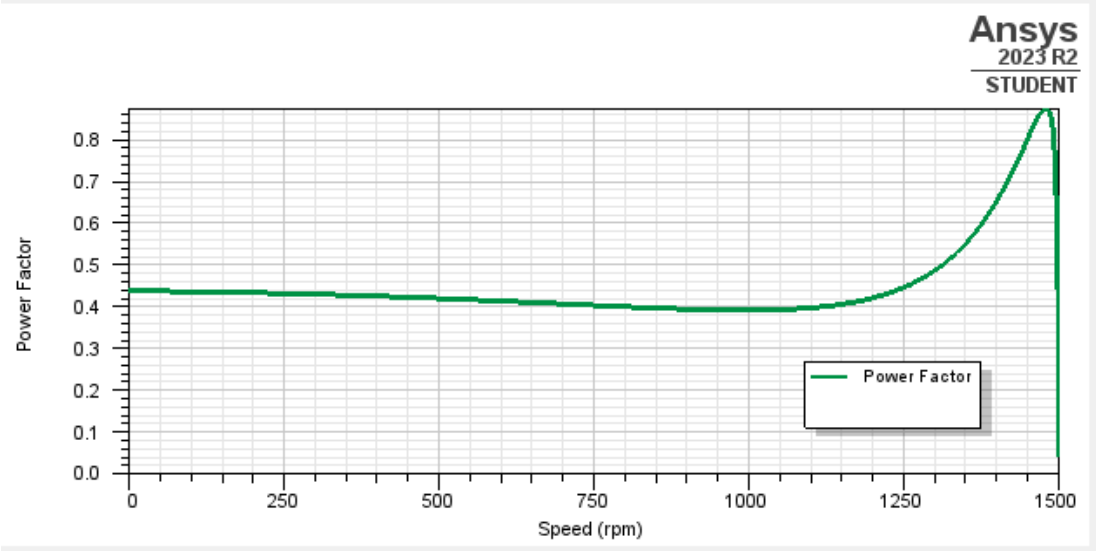

Figure 4.7: Power factor – Speed Curve

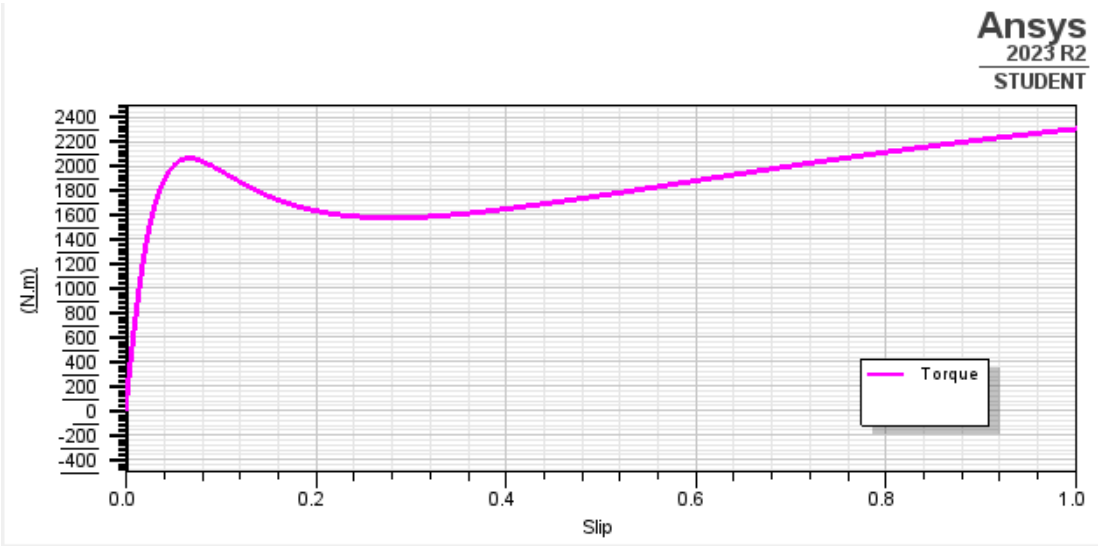

Figure 4.8: Torque-Slip Curve

Table 4.7: Reference Motor Design Solution Data

	Performance Value	
	Reference Motor Design Solution	**Test**
Output Power(kW)	109,99kW	110,1kW
Efficiency (%)	95,11%	94.65%
Power Factor	0,860	0.862
Rated Shaft Speed (rpm)	1485,0	1489,0
M_k/M_n	3,25	2,14
I_k/I_n	7,75	6,16

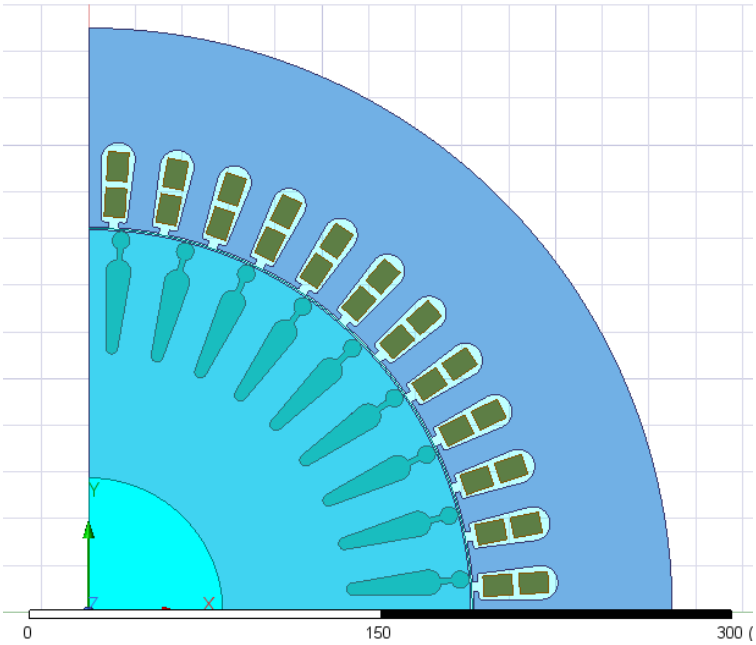

Figure 4.9: 2D Model of the Reference Motor in ANSYS Maxwell

Upon comparing the reference motor's modelling with the analysis and test results, it is evident that the efficiency value is low, placing it in the IE2 efficiency

class. To increase efficiency from IE2 to IE4, designs have been proposed with the aim of minimizing costs. The analysis results of the reference motor indicate that the highest iron loss is shown in Table.

Table 4.8: Reference Motor Losses Analysis Solution

Losses	Value
Copper Loss of Stator Winding (W):	1530.12
Copper Loss of Rotor Winding (W):	1114.88
Iron-Core Loss (W):	1823.19
Frictional and Windage Loss (W):	626.65

Table 4.9: Reference Motor Current Analysis Solution

Stator Current Density (A/mm²):	368.383
Specific Electric Loading (A/mm²):	353.166
Stator Thermal Load (A²/mm³):	130.1

Table 4.10: Comparison Table of Datasheet of Reference Motor and Test Data

Parameter	Data	Test
Voltage	380 V	373 V
Phase Current	197,7 A	213,1A
Frequency	50 Hz	50 Hz
Rpm	1486rpm	1489d/dk
Output Power	110 kW	110,1 kW
Efficiency	%94,5	%94,65
Power Factor	0,85	0,862
M_k/M_n	2,4	2,14
I_k/I_n	6,7	6,16

4.1 EXPERIMENTALRESULTS OF THE REFERENCE MOTOR

After producing the reference motor designs using ANSYS Maxwell, Table 4.11 presents a comparison of the analysis results with the test results.

Table 4.11: Design Value vs Test Value

Parameter	Design Value	Test Value
Voltage	380	373
Efficiency	95,04	94,65
Mn	707,283 Nm	706 Nm
Rpm	1486	1485
Power Factor	0,835	0,861
Stator Copper Loss	1,5kW	2,32kW
Iron Loss	1.97kW	1.34kW
Rotor Conductor Loss	1,14kW	1,14kW
Mechanical Loss	0,627kW	0,924kW
Total Loss	5,73kW	6,34kW

In evaluating the comparison, distinctions between design and test become apparent, forming the design-test ratio. In evaluating the comparison, distinctions between design and test become apparent, forming the design-test ratio. Use of this ratio in forthcoming studies can simplify the prediction of actual outcomes. As demonstrated here, decreasing the losses of the motor enhances efficiency. Our primary aim is to optimize parameters and decrease losses.

4.2 FINITE ELEMENT METHOD OF REFERENCE MOTOR

The Finite Element Method (FEM) is a numerical approach used to simulate and solve problems related to engineering, physics and other scientific fields. In electrical engineering, FEM is used to simulate the locally degraded permeability of electrical steel laminations when subjected to cutting effects in simulations [1]. There are two typical approaches to implement cutting effect - zone-based and local-based models. The local-based approach realizes continuous local material properties, whereas the zone-based model subdivides the iron core of a model into a few slices parallel to a cut edge [1]. FEM involves assigning different material properties such as BH curve and iron-loss coefficient to cope with deteriorations near the cut edge [1]

Finite Element Method (FEM) analysis is a valuable tool in the design and optimization of IE4 induction motors. By utilizing FEM analysis, designers can obtain insights into the electromagnetic and thermal behavior of the motor, which facilitates the optimization of the motor's design [2]. FEM analysis also enables designers to identify weak spots in the design of IE4 induction motors, which might lead to mechanical failure or suboptimal performance. This helps in improving the overall reliability and performance of the motor [2]. Additionally, FEM analysis allows designers to evaluate the performance of the motor under different operating conditions, such as varying loads and speeds. This helps in determining the motor's efficiency and power factor, which are crucial parameters for the successful operation of IE4 induction motors in various applications [2]. Therefore, FEM analysis provides an efficient and accurate way to optimize the design of IE4 induction motors, ensuring that they meet the required specifications for high efficiency and reliable operation.

The stator and rotor geometries of the reference motor have been inputted into the ANSYS Maxwell 2D sofware for finite element analysis. The surfaces selected for analysis were created within a 2D environment. Material data, including the B-H curve and material loss coefficients, have been imported into the program. The finite element

method is widely utilized across various fields. The use of the finite element method and the corresponding analysis programmers is commonplace in observing saturation effects that can occur in magnetic circuits, particularly. Figure presents the 2D model that should be utilized when applying the finite element method.

Finite element analyses of the EMTAŞ branded induction motor, whose design was verified as a result of analytical analyses, were performed.

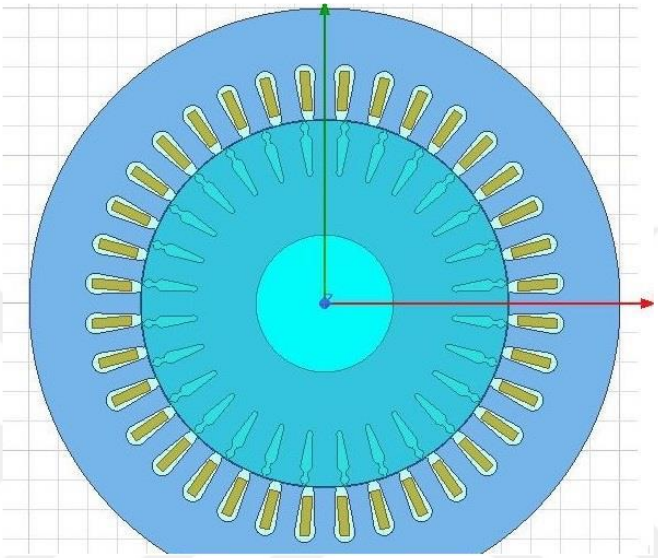

Figure 4.10: 2D Model of the Geometry in ANSYS Maxwell

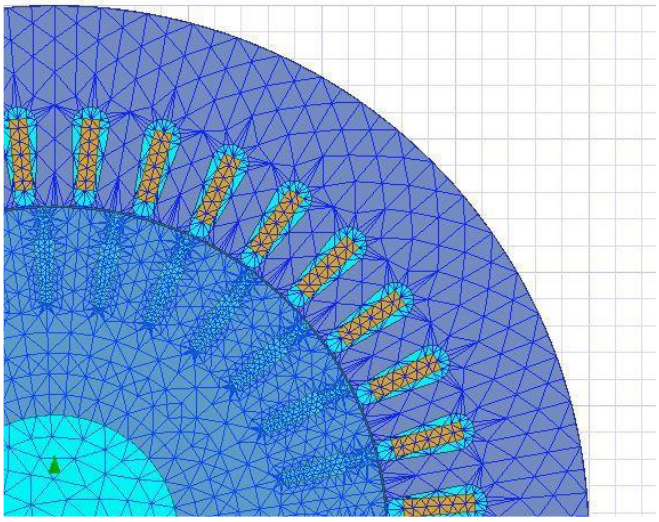

Figure 4.11: Maxwell 2-D Mesh Structure

The model's mesh structure, to which the finite element method will be applied, is presented in Figure.

The flux change in the outer regions of the stator will not occur rapidly, allowing for a wider mesh structure. However, due to the fast magnetic flux changes in the air gap, a tighter mesh structure should be used for the tooth tips and air gap. Refer to Figure 4.11 for the air gap mesh structure.

CHAPTER V
PARAMETER-BASED DESIGN OF A 110 KW 4-POLE INDUCTION MOTOR

The chapter presents innovative designs, and the final design suitable for the thesis purpose has been processed and produced. The experimental results of the real induction motor will be compared with the design results of the final design. The 4th design shows the impact of the changes in the motor's structures on the parameters. The 5th design is a combination of the other designs and represents the final configuration. The initial step in manufacturing the motor involves printing the laminations of the stator and rotor slots on silicon sheets, which are selected based on the quality of the silicon sheet. For the rotor manufacturing process, aluminum is injected into the rotor slots using injection presses, according to the created stack, and the shaft is then passed through with the help of the press. This results in the rotor stack being ready for the assembly stage. In the same way, the stack created for the stator goes to the coil winding section and the stator windings are wound.

5.1 DESIGN I

In this design, the stator and rotor geometries remain unchanged, but various silicon sheets were utilized to investigate iron losses. To diminish iron losses, M400-50A and M330-50A silicon steel sheets were implemented instead of M530-50A. B-H curves for each type of sheet are presented in Figures 5.1, 5.2, and 5.3 for M530-50A, M400-50A, and M330-50A, respectively.

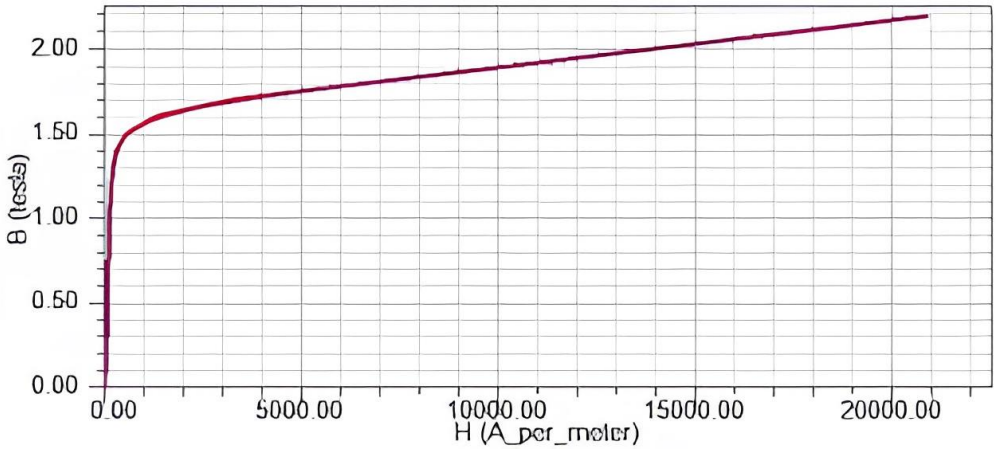

Figure 5.1: M530-50A B-H Curve

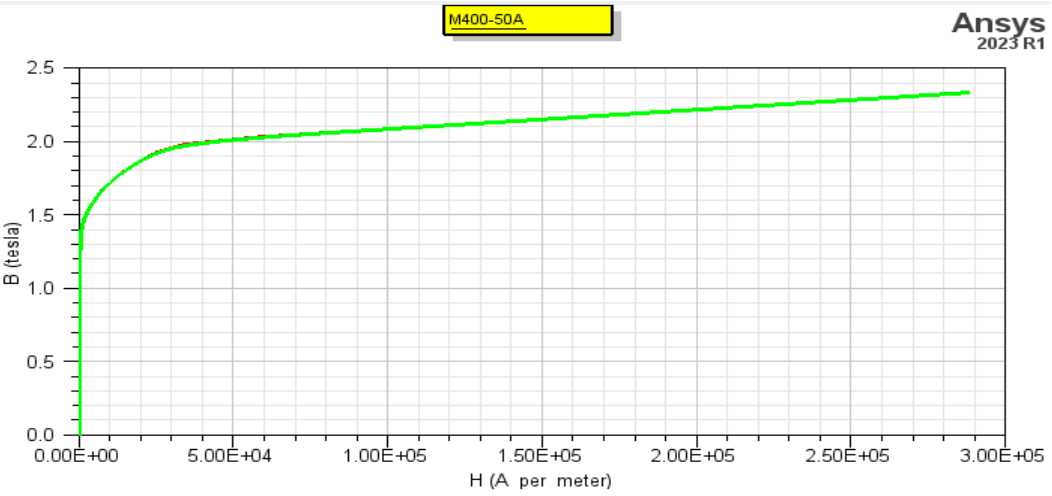

Figure 5.2: M400-50A B-H Curve

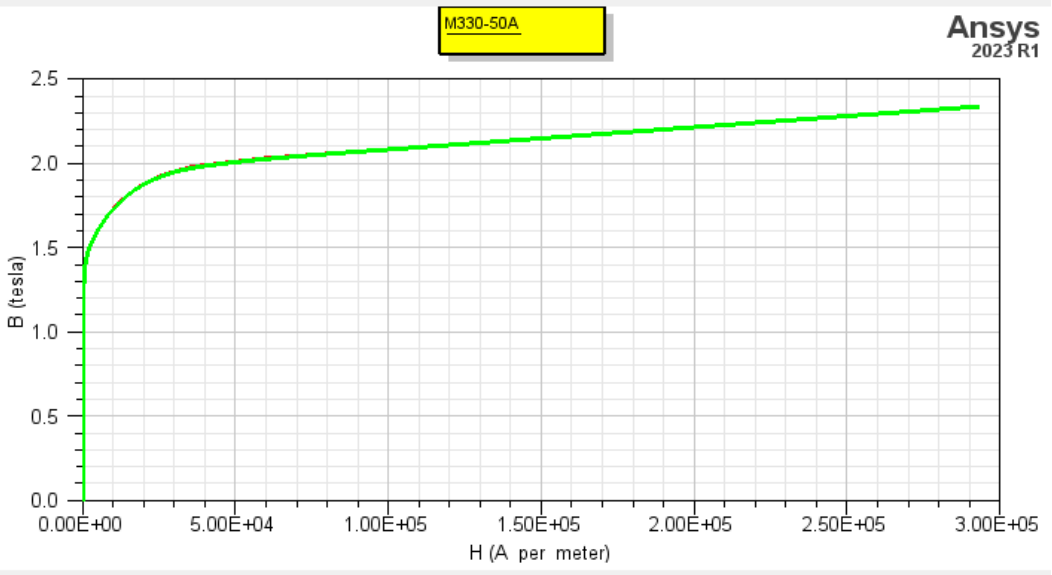

Figure 5.3: M330-50A B-H Curve

Using these sheets will reduce iron losses. Additionally, we will implement bearings with lower friction losses to further decrease inefficiencies. Although this will lead to improved efficiency, it will not quite reach our initial target. To address this, we will incorporate lamination materials in the final design to achieve the desired level of efficiency. Upon analysis, it was determined that switching to M400-50A grade silicon sheets in the reference motor would be more suitable. This grade reduces iron losses and improves efficiency compared to the more affordable M530-50A grade. M330-50A was not chosen due to significantly higher costs. Additionally, the thickness of the silicon steel sheets impacts the motor's efficiency. However, a thickness of 0.5 mm was selected to keep costs low.

Table 5.1: Design the Results Based on the Quality of the Material

Parameter	ReferenceMotor-M530-50A	ReferenceMotor-M400-50A	ReferenceMotor-M330-50A
Voltage	380	380	380
Efficiency	95,04	95,38	95,65
Mn	706,722 Nm	707,202 Nm	707,31
Rpm	1486,27	1485,04	1485,04
Power Factor	0,83	0,84	0,84
Stator Copper Loss	1,554kW	1,593kW	1,583 kW
Iron Loss	1.976kW	1.441kW	1,110kW
Rotor Conductor Loss	1,021kW	1,14kW	1,14kW
Mechanical Loss	0,627kW	0,626kW	0,626kW
Total Loss	5,73kW	5,325kW	4,98kW

Efficiency curves by material change are shown in Figures 5.4, 5.5, 5.6, 5.7, 5.8, 5.9. Current curves according to material change are shown in 5.10, 5.11, 5.12.

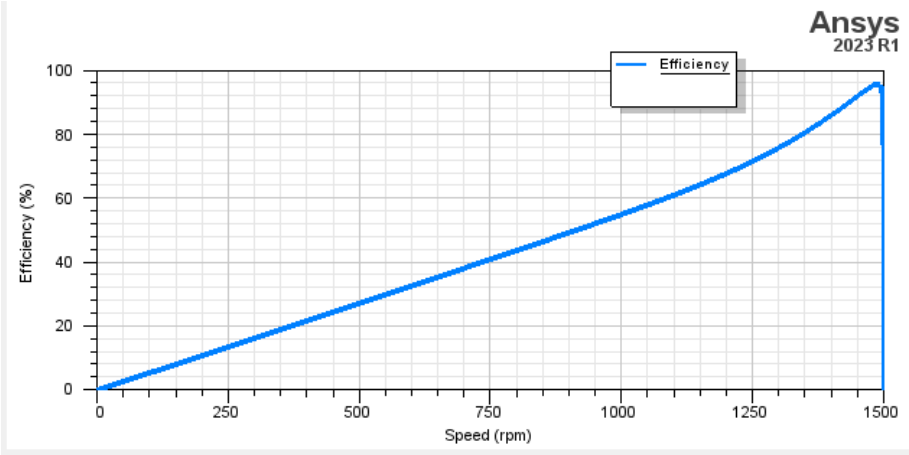

Figure 5.4: M330-50A Efficiency Graph

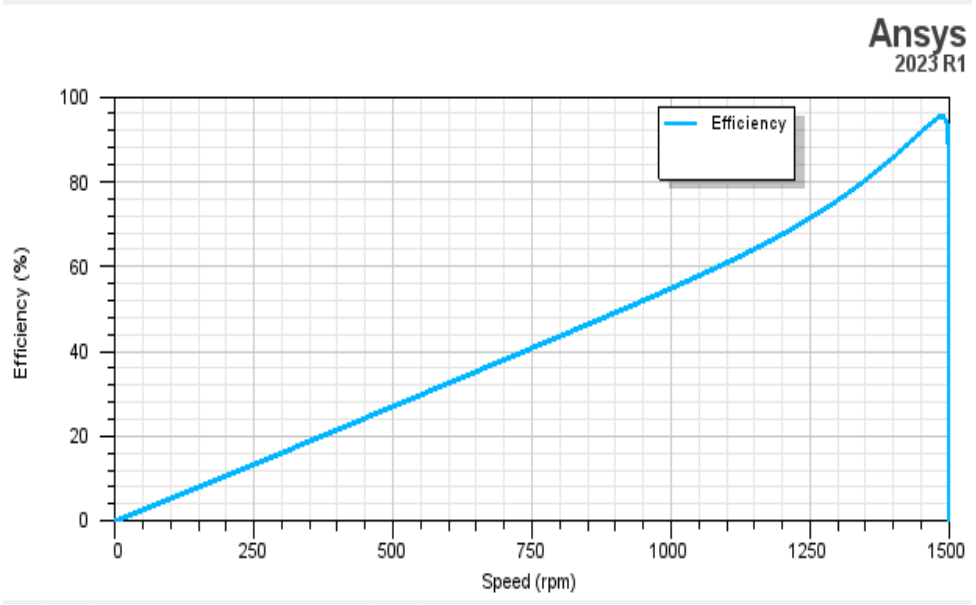

Figure 5.5: M400-50A Efficiency Graph.

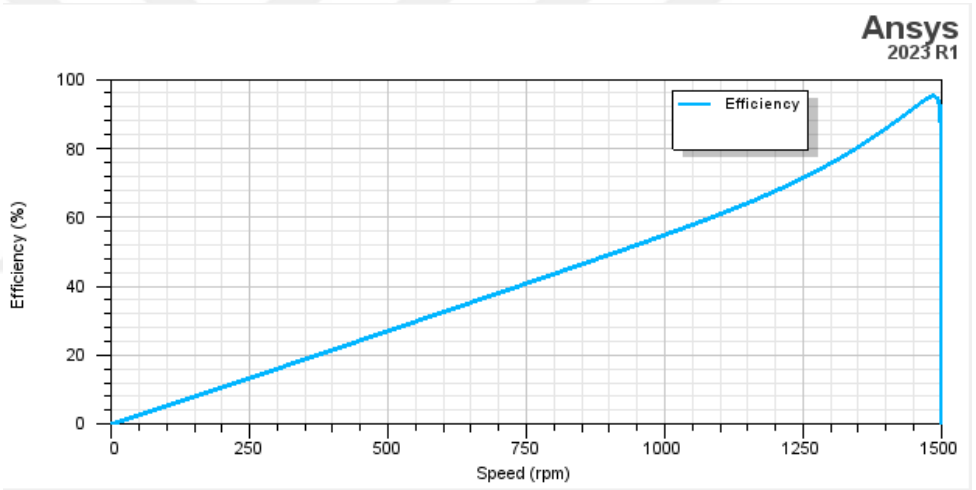

Figure 5.6: M530-50A Efficiency Graph

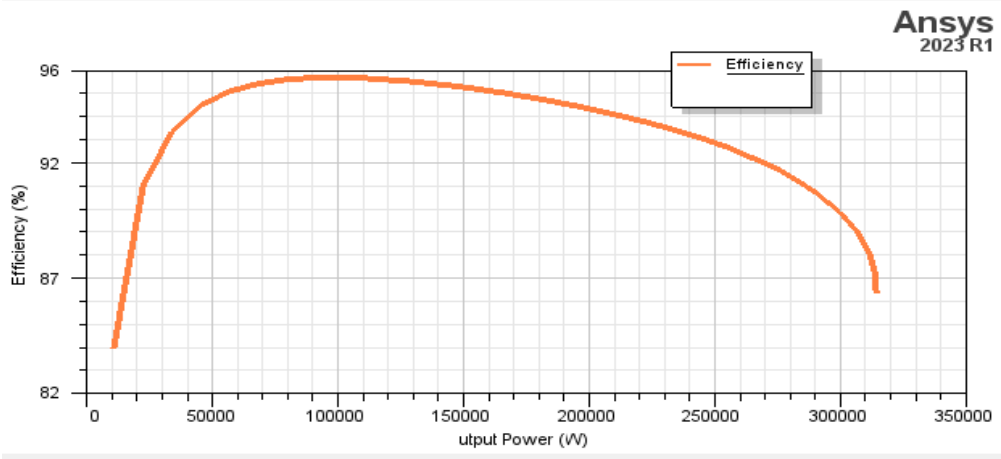

Figure 5.7: M330-50A Efficiency vs. Output Power Curve

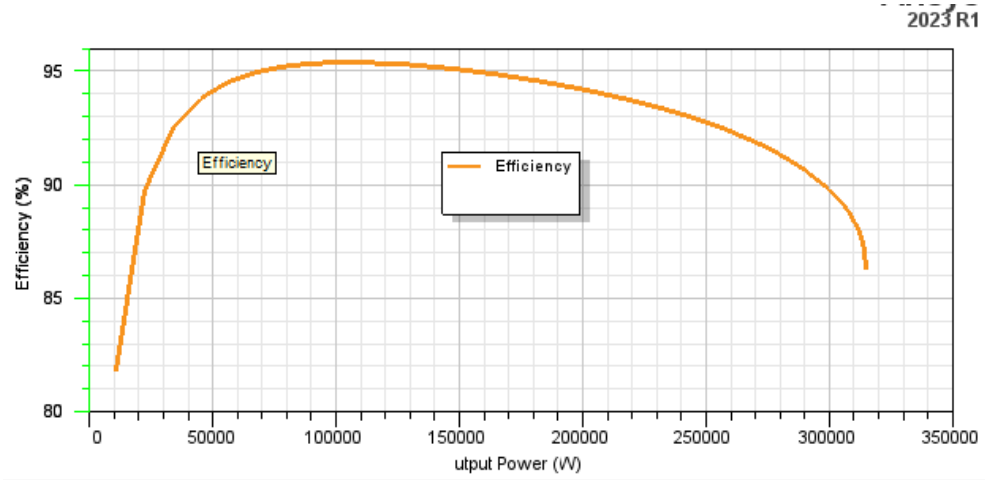

Figure 5.8: M400-50A Efficiency vs. Output Power Curve

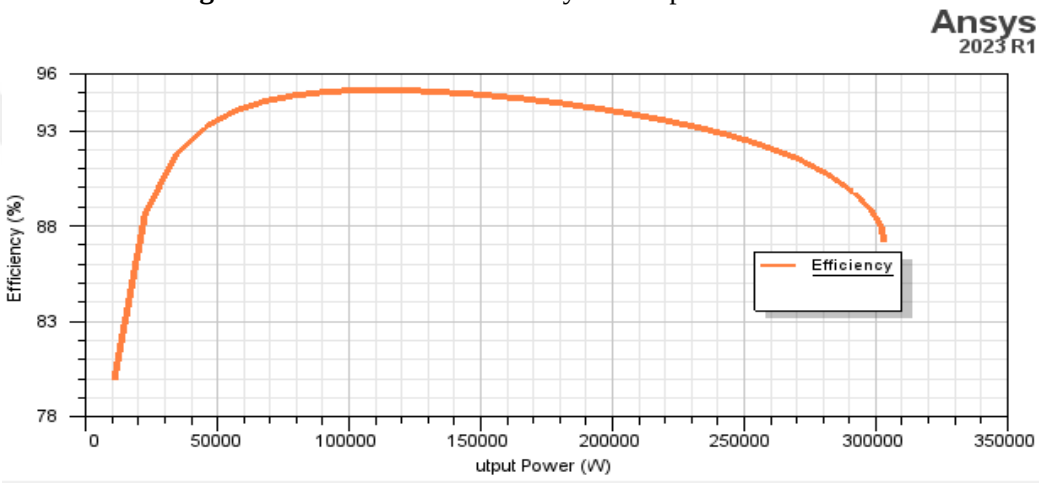

Figure 5.9: M530-50A Efficiency vs. Output Power Curve

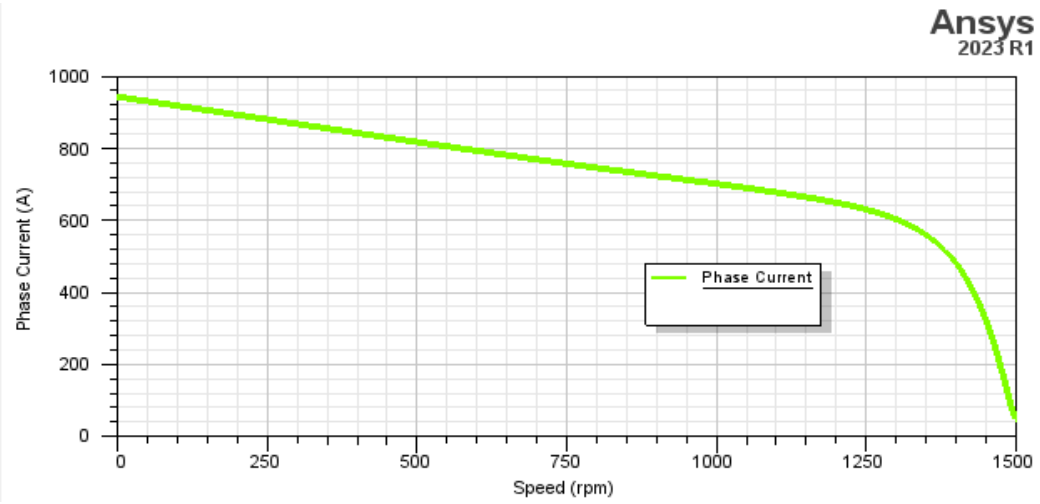

Figure 5.10: M330-50A Phase Current vs. Speed Curve

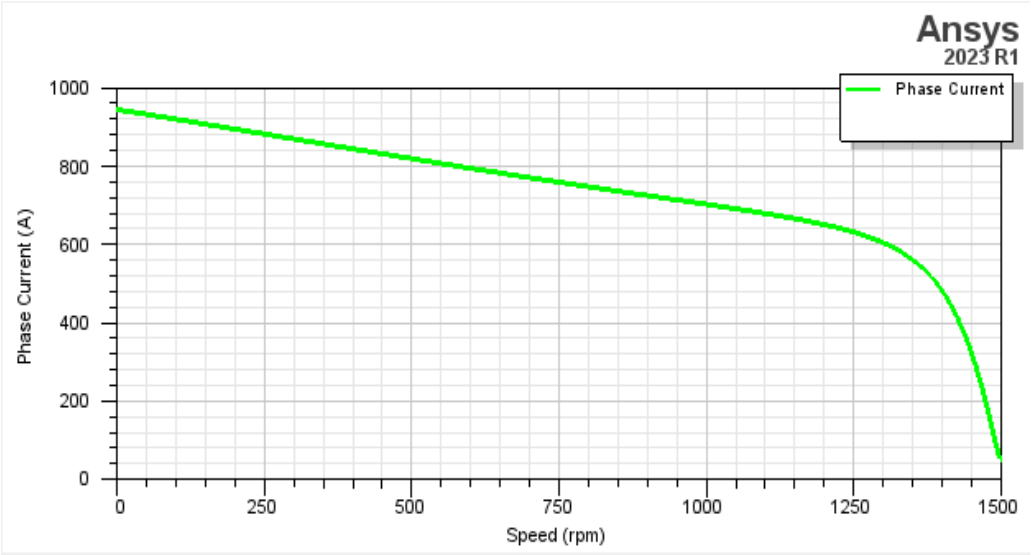

Figure 5.11: M400-50A Phase Current vs. Speed Curve

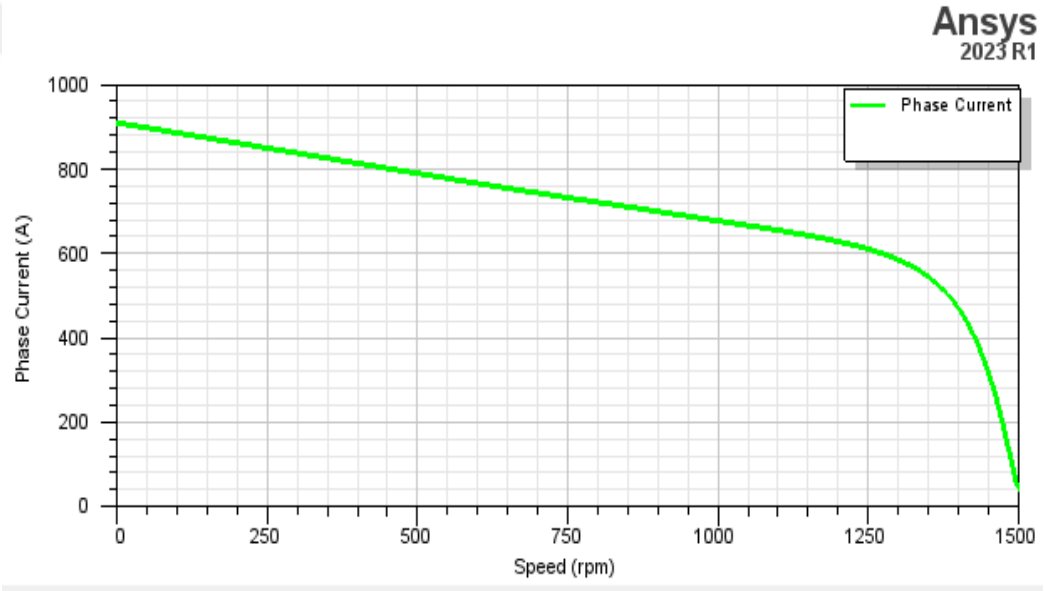

Figure 5.12: M530-50A Phase Current vs. Speed Curve

Table 5.2: Comparison of the Flux Densities

Parameter	ReferenceMotor-M530-50A	ReferenceMotor-M400-50A	ReferenceMotor-M330-50A
Stator-Teeth Flux Density (Tesla)	1.61	1.58	1.59
Rotor -Teeth Flux Density (Tesla)	1.17	1.15	1.15
Stator -Yoke Flux Density (Tesla)	1.48	1.48	1.48
Rotor-Yoke Flux Density (Tesla)	1.37	1.38	1.37
Air-Gap Flux Density (Tesla)	0.79	0.77	0.77
Stator Phase Current(A)	117.351	119.763A	119.365

When comparing the data in Table 5.2, it can be observed that the saturation of flux reduces with the enhancement of silicon sheet quality. Similarly, the thickness or thinness of the silicon sheet affects the efficiency of the motor. It is observed that the efficiency of the motor increases with its thinness; however, due to the higher cost associated with a thinner sheet, the existing stator and rotor silicon sheet with a thickness of 0.5 mm is utilized.

5.2 DESIGN II

The stator area of the reference motor is 437.158 mm². To observe the changes in parameters, the winding values will be altered while maintaining a constant stator area. The reference motor has a 12+13 turns double-layered winding consisting of 4 parallel groups, with a wire diameter of 6x1.30 mm². The uninsulated fill factor is 45.4%. In Design 2, it has been identified that the stator slots have a gap, which will require additional stator windings during the winding process. The fill factor will be enhanced by implementing this winding modification. Currently, the fill factor stands at 47.4% without insulation. Increasing the amount of winding will result in improvements in power factor and efficiency while decreasing stator and rotor flux densities as well as stator phase current. Deviations from the optimal winding ratio of the motor will lead to a decrease in the aforementioned parameters. The study examined 4 designs in depth to ascertain these outcomes.

Table 5.3: Comparison of Different Windings

Parameter	Reference Motor	Design 1	Design 2	Design 3	Design 4
Winding	12+13	13+13	13+14	12+12	11+12
Wire Size	6x1,30	6x1,30	3x1,30+3x1,25	7x1,25	8x1,20
Voltage(V)	380	380	380	380	380
Efficiency	95,04	95,11	95,09	95,00	94,83
Power Factor	0,85	0,86	0,87	0,80	0,74
Stator-Teeth Flux Density (Tesla)	1,65	1,61	1,58	1,70	1,76
Rotor -Teeth Flux Density (Tesla)	1,20	1.17	1,14	1,23	1,28
Stator -Yoke Flux Density (Tesla)	1,54	1.48	1,42	1,61	1,69
Rotor-Yoke Flux Density (Tesla)	1,43	1.37	1,31	1,50	1,57

Table 5.3 (Continued): Comparison of Different Windings

Air-Gap Flux Density (Tesla)	0,89	0.79	0,77	0,83	0,86
Stator Phase Current(A)	120,98	117.351	115,527	126,9	136,7
Copper Loss of Stator Winding (kW)	1,55	1.530	1,597	1,51	1,6
Copper Loss of Rotor Winding (kW)	1,021	1.114	1,211	0,938	0,857
Iron-Core Loss (kW)	1,97	1.823	1,692	2,11	2,35
Frictional and Windage Loss (kW)	0.627	0.626	0,625	0,628	0,629
Stray Loss kW)	0,549	0.549	0,550	0,549	0,549
Total Loss (W)	5,731	5,641	5,676	5,77	5,99
Fill Factor	45,7%	47,4%	47,4%	47,3%	47,5%

5.3 DESIGN III

In Design 3, design analyses will be conducted by varying the motor's stack length. Increasing the stator and rotor stack length will result in decreased magnetic flux density, iron losses, and stator copper losses, thereby reducing the current. Correspondingly, there will be an increase in voltage that generates the moment in the motor. However, an increase in iron losses is expected with increasing stack length. While it is anticipated that efficiency will improve with a larger stack size, it is crucial to assess other factors before deciding on the optimal stack size.

Table 5.4: Effect of Stack Length on Parameters

Parameter	Reference Motor	Design 1	Design 2	Design 3	Design 4
Length(mm)	250	210	230	270	290
Voltage(V)	380	380	380	380	380
Efficiency	95,04%	94,20%	94,74%	95,17%	95,22%
Power Factor	0,85	0,67	0,76	0,869	0,88
Moment	706,22 Nm	706,17 Nm	706,75 Nm	706,84 Nm	707,23Nm
Rpm	1486,27	1487,24	1486,93	1485,53	01484,73
Stator-Teeth Flux Density (Tesla)	1,65	1,94	1,76	1,58	1,50
Rotor -Teeth Flux Density (Tesla)	1,20	1,41	1,28	1,14	1,52
Stator -Yoke Flux Density (Tesla)	1,54	1,86	1,69	1,42	1,31

Table 5.4 (Continued) Effect of Stack Length on Parameters

Rotor-Yoke Flux Density (Tesla)	1,43	1,73	1,57	1,31	1,21
Air-Gap Flux Density (Tesla)	0,89	0,94	0,86	0,77	0,73
Stator Phase Current(A)	120,98	152,13	132,85	115,94	113,896
Copper Loss of Stator Winding (kW)	1,55	2,227	1,80	1,48	1,48
Copper Loss of Rotor Winding (kW)	1,021	0,926	0,972	1,077	1,137
Iron-Core Loss (kW)	1,97	2,38	2,149	1,83	1,70
Frictional and Windage Loss (kW)	0.627	0,628	0,628	0,627	0,626
Stray Loss kW)	0,549	0,550	0,550	0,549	0,549
Total Loss (W)	5,731	6,76	6,11	5,55	5,50

5.4 DESIGN IV

One of the critical parameter parameter that affects the performance of the induction motor is the air gap. A large or small air gap will lead to reduced motor efficiency. When selecting the optimal value of the air gap, production processes must be taken into account. Opting for a small air gap may cause problems during assembly and rotor stack rotation. An increase in the air gap results in a decrease in parameters like efficiency, speed, and power factor, while losses and phase currents may increase. Although challenges arise during the production processes when reducing air gap, there is an increase in factors such as efficiency, power factor, and speed. This slight change in cost makes it appropriate to optimize the reduction of the air gap. Material costs have remained stable, while labour time has increased resulting in assembly time rising from 30 to 45 minutes.

Table 5.5: Comparison of the Various Air Gap Lengths

Parameter	Reference Motor	Design 1	Design 2	Design 3	Design 4
Air Gap(mm)	1,325mm	1,200mm	1,100mm	1,400mm	1,500mm
Voltage(V)	380	380	380	380	380
Efficiency	95,04	95,078	95,12	95,02	95,00
Power Factor	0,85	0,846	0,863	0,823	0,820
Moment	706,22	706,993	706,677	706,77	707,81
Rpm	1486,27	1486,28	1486,31	1486,27	1486,25
Stator-Teeth Flux Density (Tesla)	1,65	1,65	1,64	1,65	1,66

Table 5.5 (Continued): Comparison of the Various Air Gap Lengths

Rotor -Teeth Flux Density (Tesla)	1,20	1,20	1,19	1,20	1,20
Stator -Yoke Flux Density (Tesla)	1,54	1,55	1,55	1,54	1,54
Rotor-Yoke Flux Density (Tesla)	1,43	1,43	1,43	1,43	1,43
Air-Gap Flux Density (Tesla)	0,89	0,92	0,94	0,82	0,80
Stator Phase Current(A)	120,98	119,39	116,94	121,85	123,19
Copper Loss of Stator Winding (kW)	1,55	1,51	1,45	1,57	1,61
Copper Loss of Rotor Winding (kW)	1,021	1,021	1,018	1,022	1,024
Iron-Core Loss (kW)	1,97	1,98	1,98	1,97	1,97
Frictional and Windage Loss (kW)	0.627	0,627	0,627	0,627	0,627
Stray Loss (kW)	0,549	0,550	0,549	0,550	0,550
Total Loss (W)	5,731	5,61	5,60	5,75	5,77

5.5 DESIGN V

After comparing the experiments conducted in Designs 1, 2, 3, and 4, a slight increase in efficiency was observed. However, by considering the experiments carried out in other designs, a high-efficiency motor can be produced. Therefore, new stator and rotor dimensions were designed for Design 5.

The dimensions of the reference motor were entered into the ANSYS Maxwell program to determine Hs0 (slot mouth height), Hs1 (radius), Hs2 (slot height), Bs0 (slot mouth width), Bs1 (slot lower width), and Bs2 (slot upper width). The slot structures of the reference motor were created in previous designs, and multiple design trials were conducted to develop the optimal new slot structure. The rotor structure has double-cage slot double corrugated, and optimal designs were made by examining the upper and lower dimensions separately. The designs included optimization of both rotor and stator slots. For the rotor corrugations, the height was kept constant while the width values were optimized. Then, the width dimensions were kept constant while the height values were optimized. To maintain a constant fill factor, changes have been

made to the winding structure, such as the amount of wire used, wire thickness, and insulation, due to the impact of changes in the stator slot structure. Despite minor adjustments in the optimized version, efforts have been made to improve efficiency. When designing a motor, the dimensions of the stator and rotor slots are crucial parameters. To compare a single deep slot design with a double cage slot design, the volumes of the slots were kept constant. This allowed us to observe the difference while keeping the rotor slot resistance constant. In this design, only the rotor slots were changed while the stator dimensions, stator slot dimensions, material type, and stack length remained the same. Changes were also made to the stator windings, specifically in the number of turns, amount of wire, and wire diameters while maintaining the same fill factor Cost was taken into consideration during these changes to ensure the most cost-effective solution. This study compares the double-layered winding and single layered winding techniques, using different numbers of wires. The performance effects of the windings on the motor were observed through unloaded and loaded operation experiments. The results indicate that increasing the number of turns generally increases the Cosφ value. This study observed that the winding structure, number of turns, and wire properties significantly affect efficiency. Additionally, the number of revolutions decreases during motor loading experiments, with a corresponding decrease in the number of turns. As a result, the nominal slip value also increases. The optimal number of turns can be determined by comparing the results obtained from finite element analysis with experimental data and optimizing the latter.

Increasing the slot areas has reduced both stator and rotor copper losses, and due to the decrease in stack length, it has also caused a decrease in iron losses. Increasing the rotor slot area reduces rotor resistance and increases the motor's rated speed. It is expected that the starting torque and current will decrease as well.

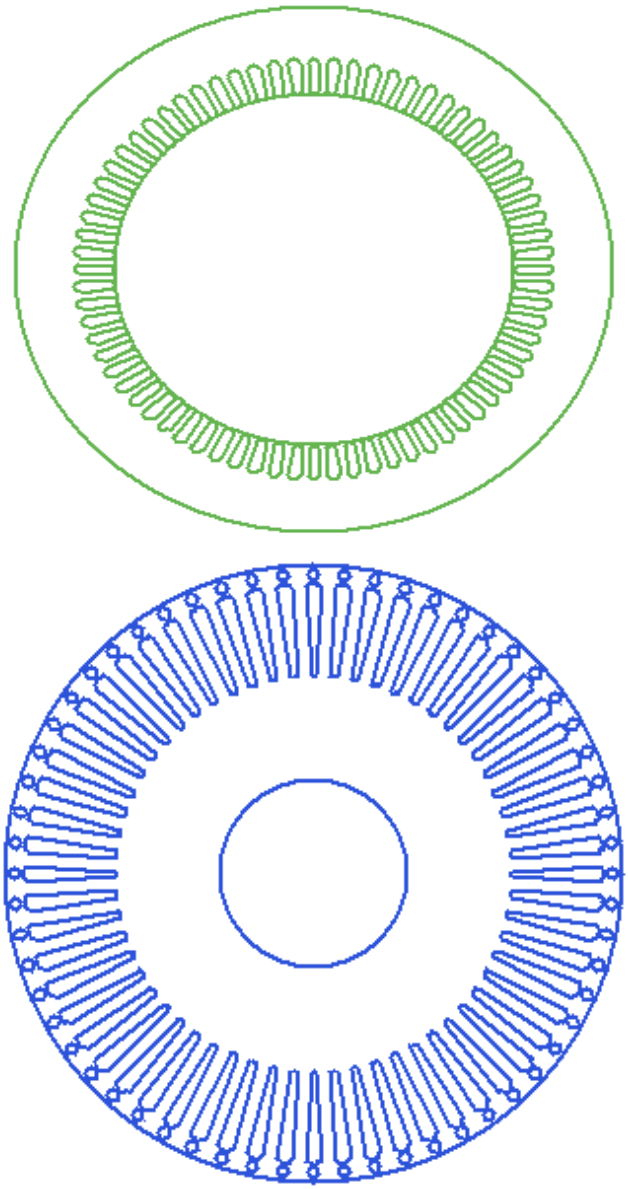

Figure 5.13: Stator and Rotor Geometry of Design V Motor

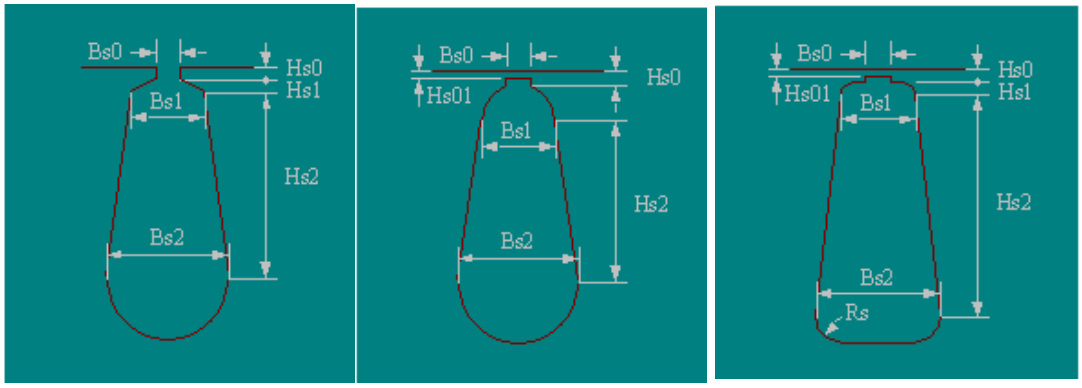

Figure 5.14: Representation of Dimensions of Stator Slot (a), Rotor Slot (b), and Rotor Bottom Slot (c)

Table 5.6: Stator Slot Dimensions

Parameter	Stator Slot
Hs0 [mm]	0,71
Hs1 [mm]	2
Hs2 [mm]	30
Bs0 [mm]	3,15
Bs1 [mm]	9
Bs2 [mm]	12

Table 5.7: Rotor Slot Dimensions

Parameter	Rotor Slot
Hs0 [mm]	1.95
Hs01 [mm]	0
Hs2 [mm]	0,01
Bs0 [mm]	2,25
Bs1 [mm]	7,85
Bs2 [mm]	7,85

Table 5.8: Dimensions of Rotor Bottom Slot

Parameter	Rotor Bottom Slot
Hs0 [mm]	1.5
Hs1 [mm]	2
Hs2 [mm]	53
Bs0 [mm]	1.5
Bs1 [mm]	10
Bs2 [mm]	4.5

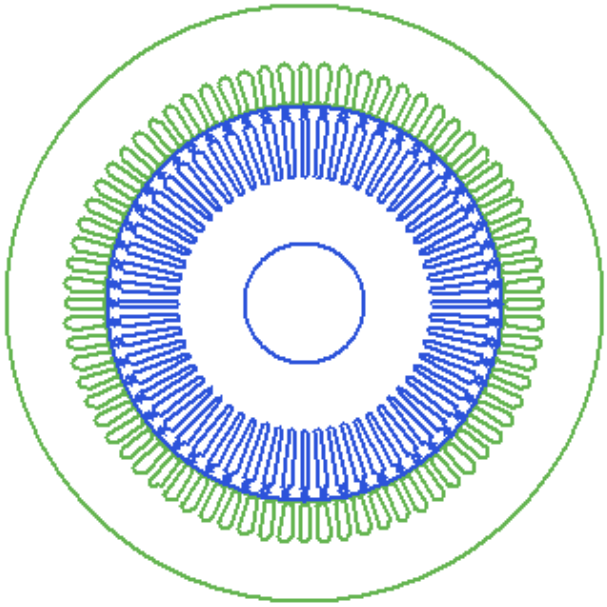

Figure 5.15: Stator and Rotor Geometry RMXPRT

The study presents the design results of the induction motor as follows.

Table 5.9: Stator-Rotor New Slot Design Solution

Parameter	Reference Motor	Final Design
Length(mm)	250	230
Voltage(V)	380	400
Efficiency	95,04%	96,73%
Power Factor	0,85	0,90
Moment	706,22 Nm	703,902 Nm
Rpm	1486,27	1491,23
Stator-Teeth Flux Density (Tesla)	1,65	1,48
Rotor -Teeth Flux Density (Tesla)	1,20	1,19
Stator -Yoke Flux Density (Tesla)	1,54	1,28
Rotor-Yoke Flux Density (Tesla)	1,43	0,59
Air-Gap Flux Density (Tesla)	0,89	0,72
Stator Phase Current(A)	120,98	104,38
Copper Loss of Stator Winding (kW)	1,55	1,36
Copper Loss of Rotor Winding (kW)	1,021	0,646
Iron-Core Loss (kW)	1,97	1,2
Frictional and Windage Loss (kW)	0.627	0,500
Stray Loss (kW)	0,549	0,549
Total Loss (W)	5,731	3,70

Graphs of the analysis results are given in Figure 5.16, Figure 5.17, Figure 5.18, Figure 5.19, Figure 5.20 and Figure 5.21.

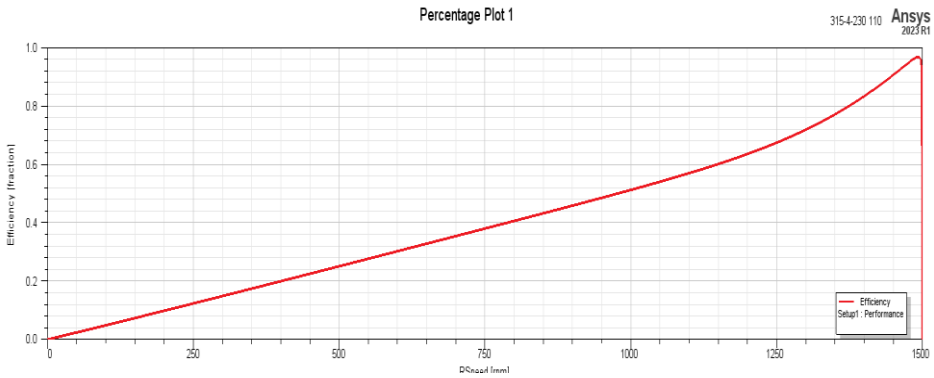

Figure 5.16: Efficiency – RPM Curve Graph

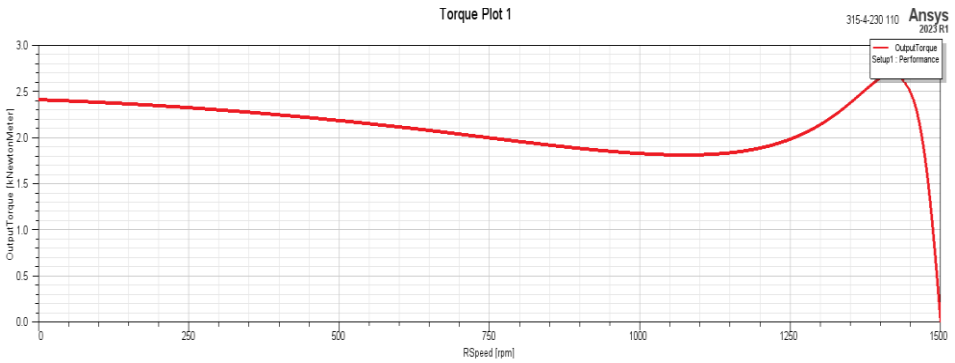

Figure 5.17: Output Torque – RPM Curve Graph

.

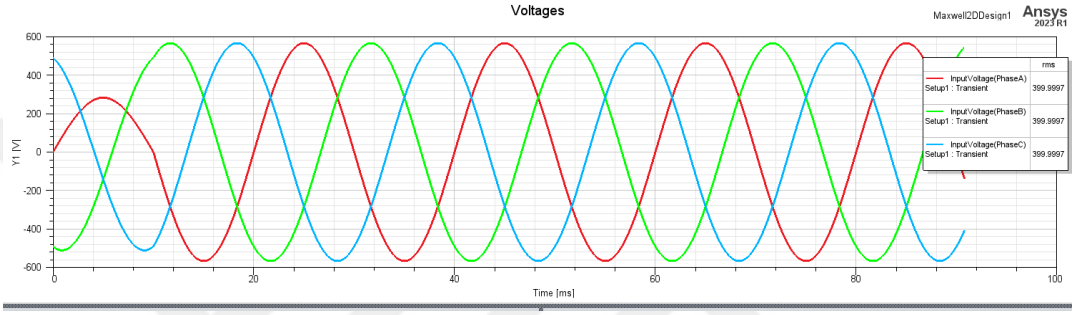

Figure 5.18: Input Voltage-Time Graph

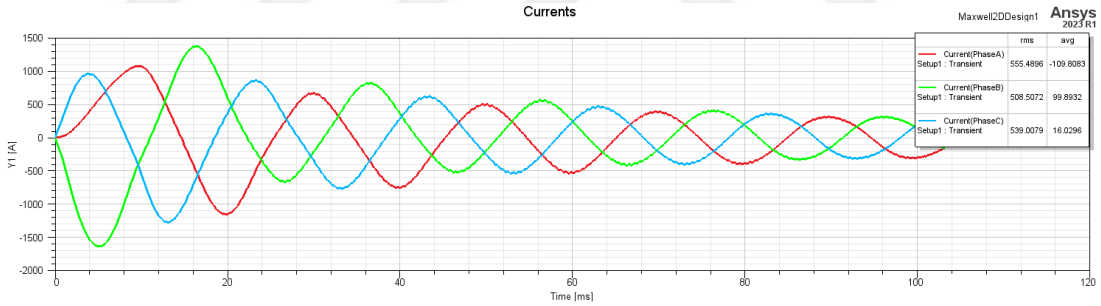

Figure 5.19: Current-Time Graph

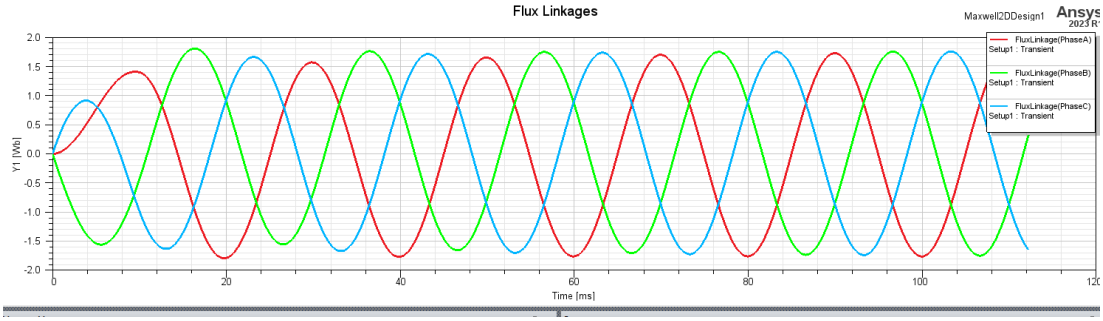

Figure 5.20: Flux Linkage-Time Graph

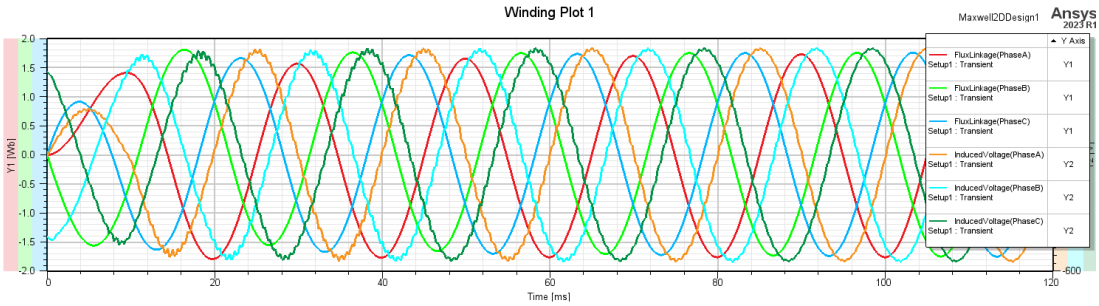

Figure 5.21: Flux Linkage and Induced Voltage-Time Graph

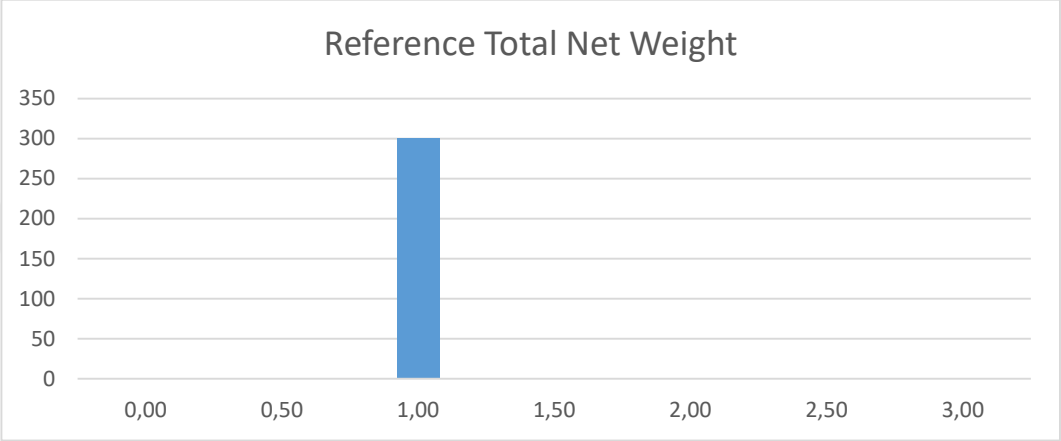

Figure 5.22: Total Net Weight(kg) -Reference Motor

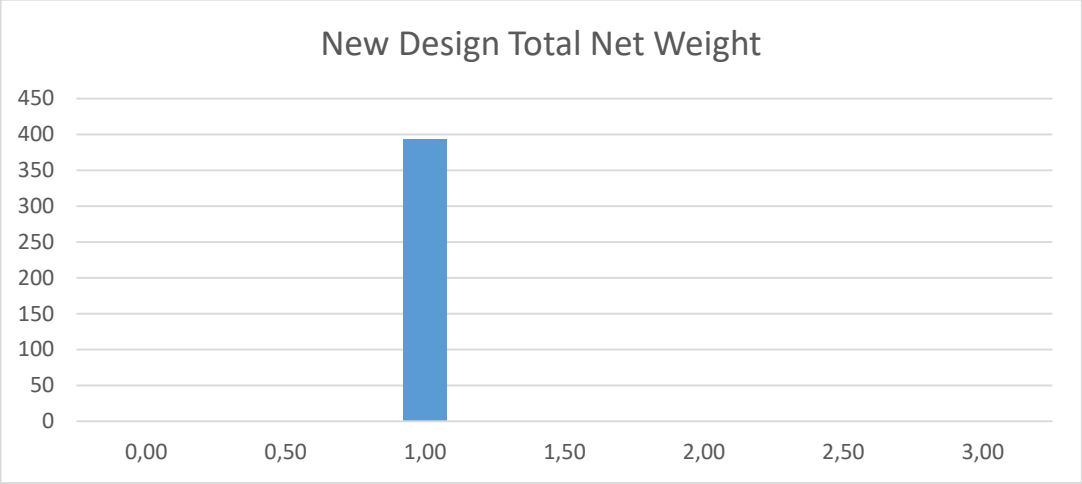

Figure 5.23: Total Net Weight(kg) -New Design Motor

While the reference motor weighed 300 kg, the total weight after the improvement was 393 kg. In terms of cost, since the weight increase is 30.99%, although the price of the product increases, it is at a tolerable rate since it provides yield improvement. The graphs can be found in sections 5.22 and 5.23. The results of the analysis are given in Figure 5.24, Figure 5.25 and Figure 5.26.

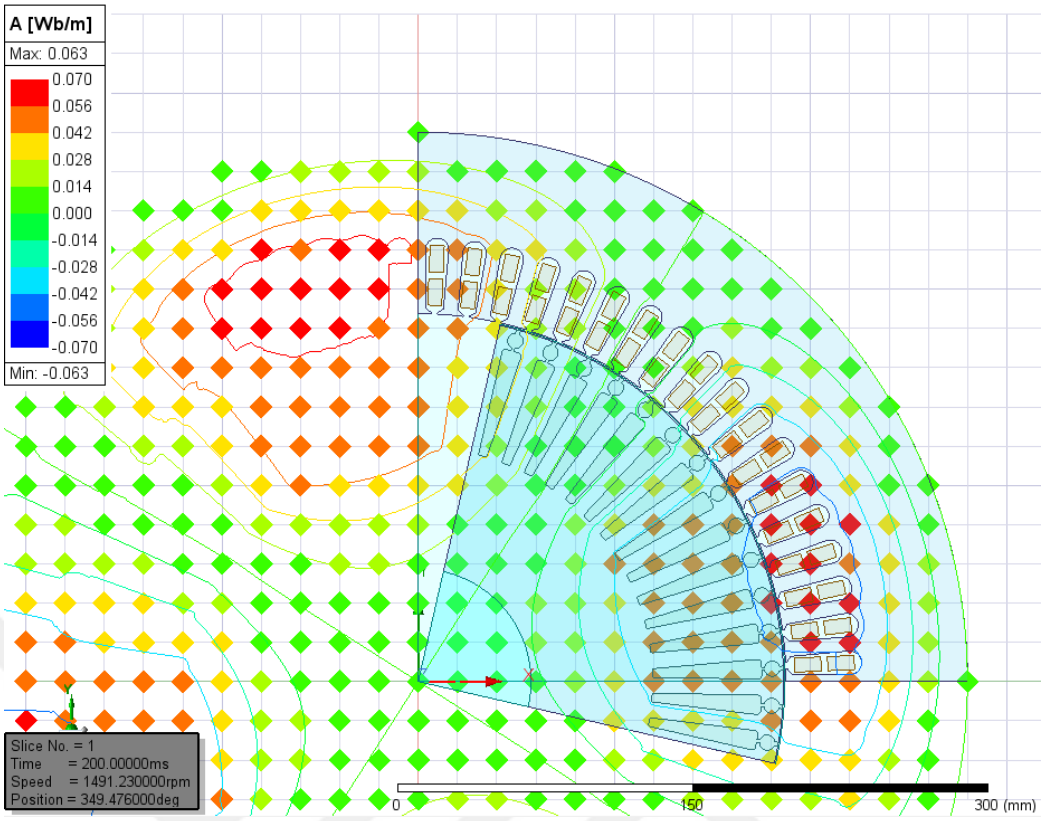

Figure 5.24: Flux Line Distribution in Maxwell 2D

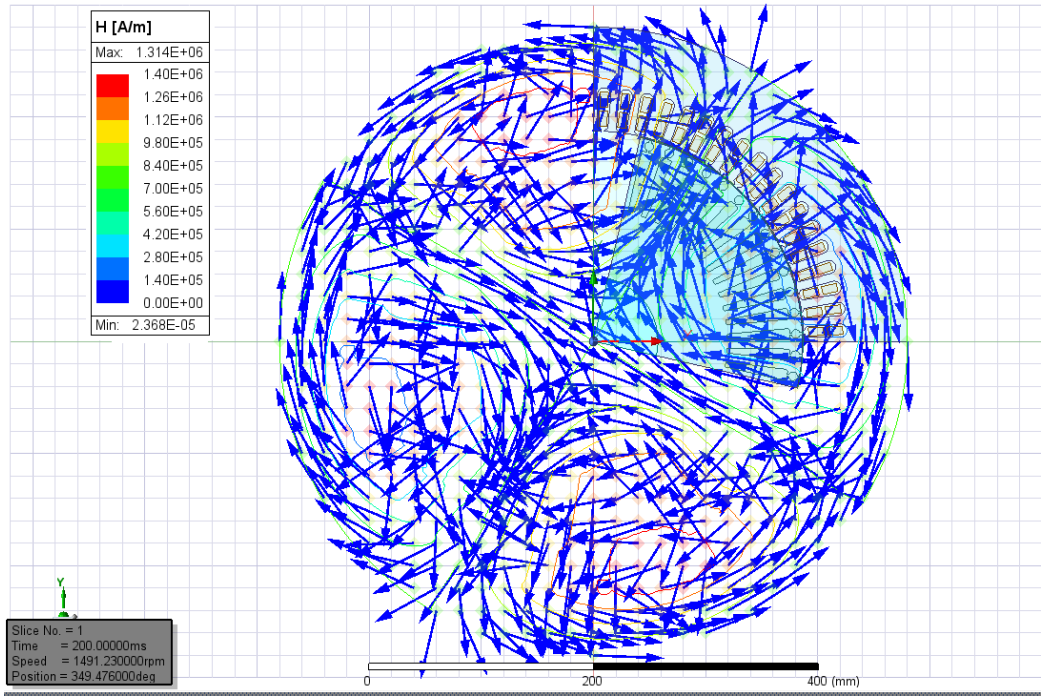

Figure 5.25: Magnetic Field Intensity Distribution in Maxwell 2D

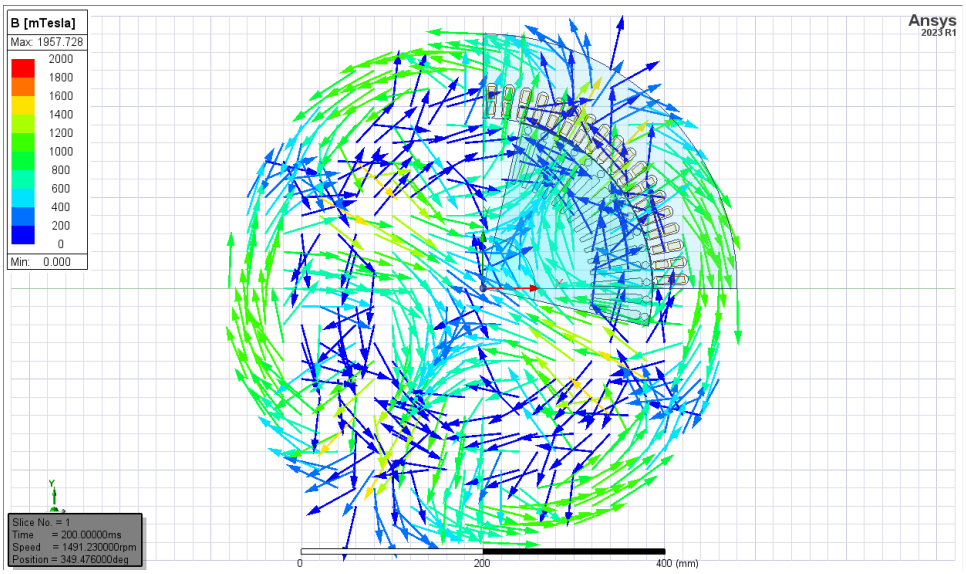

Figure 5.26: Magnetic Flux Density Distribution in Maxwell 2D

Following the completion of the electromagnetic design, the mechanical design phase commenced. Figure 5.26 illustrates the studies related to mechanical design.

Figure 5.27: 3D Renders of partial view-partial cross-section of motor (a), Outer Section of the motor (b), stator slot (c).

Figure 5.27 shows the final version of the motor, which was produced using data obtained from Design 5.

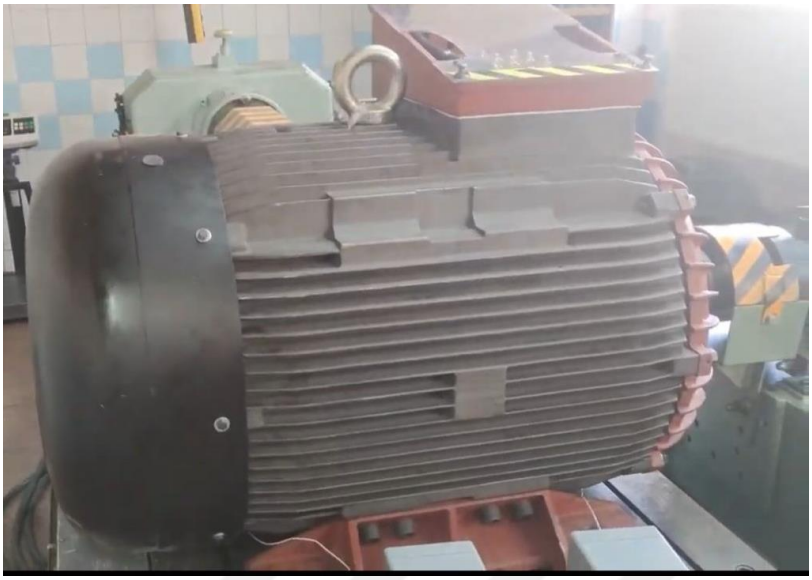

Figure 5.28: Prototype Induction Motor.

Table 5.10, Table 5.11, Table 5.12, Table 5.13, Table 5.14 and Table 5.15 below presents the test results obtained by the EMTAS Test Laboratory.

Table 5.10: Designation of Prototype Motor

Motor:315/4-230
Power:110 kW
Voltage:400 Volt
ST Ø:375
RT Ø:372,5
Stator Slot Number:72
Rotor Stator Number:60
Cooling:180/4 Plastic propeller
Silicon Steel: M400-50A

Table 5.11: Table of Laboratory Test Results

	PT 100	**(R-S) mW**	**TIME**	**V/VOLT**	**I/AMPER**	**F Hz**	**N 1/min**	**Active Power kW**	**Reactive Power kVAR**	**Output /kW**	**Cos**	**EFF/ %**	**Loss /kW**
No Load	w/o fan			400,6	42,17	50	1500	1,74	29,24	-	0,060	-	1,74
	With fan			399,5	42,1	50	1500	1,84	29,05	-	0,063	-	1,84
Cold	17,0	27,42	08:15	409,7	183,2	50	1491,0	117,80	54,70	110,2	0,907	93,57	7,58
Warm	89,0	35,36	14:15	**401,9**	**185,9**	50	**1488,0**	117,90	53,00	**110,0**	**0,912**	93,30	7,90
	Eff:%96,16												

Table 5.12: Motor No Load Test Results

U (Volt)	$(U/Un)^2$	I (A)3	P (kW)	Pcu (I^2*R) (kW)	Pfe+Pmech (kW)	Pfe (kW)	CosØ
178,8	0,199809	16,92	0,766	0,00785	0,75815	0,26915	0,146184
252,9	0,39974	24,18	1,05	0,016032	1,033968	0,544968	0,099134
309	0,596756	31,2	1,31	0,026692	1,283308	0,794308	0,078451
358	0,801025	35,62	1,61	0,03479	1,57521	1,08621	0,072893
379,3	0,899178	38,46	1,75	0,040559	1,709441	1,220441	0,06926
400,1	1,0005	41,7	1,88	0,04768	1,83232	1,34332	0,065057
418	1,092025	44,89	1,97	0,055254	1,914746	1,425746	0,060615
437,8	1,19793	48,98	2,13	0,065782	2,064218	1,575218	0,057349

Table 5.13: Indirect Method Test Results

rpm(1/min)	Rpm	1488,005
P_{cu1} (kW)	Stator copper losses	1,187342
P_{fe} (kW)	Iron losses	1,34332
P_2 (kW)	Additional losses 0,5 % from Pn acc.	0,589
P_{stat} (kW)	Total stator losses	3,119661
P_d (kW)	Power in air gap between stator and rotor	114,6803
P_{cu2} (kW)	Rotor conductor losses	0,917064
P_{mech} (kW)	Mechanical Losses	0,489
P_{rotor} (kW)	Total rotor losses	1,406064
P_{tot} (kW)	Total motor losses	4,525725
$\%\eta$	Efficiency motor	96,15813
CosØ	Power factor	0,905914
P_{out} (kW)	Output power	113,2743

Table 5.14: Slip Results

Cold slip:	9	rpm
Warm slip:	12	rpm

Table 5.15: Temperature Rise

R_t Temp Rise:	71,6	K
S_t Temp Rise:	64,1	K

The test was repeated at the electric motor laboratory of the Turkish Standards Institute, and the results are presented in the table below.

Table 5.16: Designation of Motor (by TSE)

1. Sample Information						
Power kW	**Phase-Connection**	**Voltage (V)**	**Current (A)**	**Frequency (Hz)**	**Revolutions (rpm)**	**Cos**
110	3-	400	-	50	1488	0,91
Brand	**Model**	**Serial No**	**Year of Manufacture**	**Type of Operation**	**Protection Class**	**IE**

EMTAŞ	ARGE	-	2021	S1	IP66	96,16

Table 5.17: Motor Nominal Load Test Result

2.3 Nominal Load Test (S1 warm-up test)								
S1	**U**	**I**	**P1**	**Cosø**	**n**	**T**	**P2**	**F**
Value	400,4	182,4	114,876	0,908	1488	706,752	110,112	50
Unit	V	A	kW		rpm	Nm	kW	Hz

Table 5.18: Motor Variable Load Test Result

2.4 Variable Load Test (LC)							
Loading Ratio	**Unit**	**125%**	**115%**	**100%**	**75%**	**50%**	**25%**
LC	kW	137,488	126,494	110,007	82,507	54,993	27,494
U	V	399,7	399,8	399,9	400	400,2	399,4
I	A	231	211,52	182,68	138,19	96,3	60,4
Cosø		0,904	0,907	0,908	0,899	0,859	0,702
n	rpm	1484	1485	1488	1491	1494	1497
f	Hz	50	50	50	50	50	50
T	Nm	884,706	813,178	706,132	528,389	351,445	175,361
P2	kW	137,488	126,494	110,007	82,507	54,993	27,494
P1	kW	144,546	132,83	114,832	86,072	57,311	29,325

Table 5.19: Motor No Load Test Results

2.5 No Load Test (NL)								
No-Load	110%	100%	95%	90%	60%	50%	40%	30%
U (V)	440,3	398,4	380,9	380,9	239,5	199,8	159,5	120,4
I (A)	49,2	51,16	42,74	42,74	34,88	30,27	18,8	12,02
Cosø	0,045	0,046	0,056	0,056	0,059	0,081	0,129	0,232
F (Hz)	50	50	50	50	50	50	50	50
P1 (Kw)	1,697	1,62	1,593	1,593	1,508	0,867	0,657	0,583
Q1 (kVA)	12,432	-11,898	-9,387	-9,387	8,45	1,037	1,948	0,776
S1 (kVAr)	37,527	35,307	28,197	28,197	31,786	10,47	5,194	2,507

Table 5.20: Motor Efficiency Test Result

2.6 Efficiency Calculations							
Loading Ratio	Unit	125%	115%	100%	75%	50%	25%
P2	kW	137,488	126,494	110,007	82,507	54,993	27,494
P1	kW	144,546	132,83	114,832	86,072	57,311	29,325
P1ϑ	kW	144,531	132,817	114,823	86,066	57,307	29,324
Ps ϑ	W	2855,589	2394,218	1785,863	1020,201	494,632	194,232
Pr ϑ	W	1495,23	1255,235	915,396	496,835	214,985	52,285
PLL	W	1283,006	1083,932	817,339	457,656	202,463	50,408
Pfe	W	1022,843	1022,843	1022,843	1022,843	1022,843	1022,843
Pfw	W	447,239	448,29	450,022	452,588	454,936	457,215
PT	W	7103,906	6204,518	4991,463	3450,122	2389,859	11776,982
EFF		95,10%	95,30%	95,70%	96,00%	95,80%	93,90%

When the test results performed at TSE and the electrical laboratory are evaluated, it is clearly seen that the motor falls into IE4. Studies show that improving any of the parameters helps the motor improve efficiency. At TSE, a test was conducted without any propeller improvements. Subsequently, the propeller was modified, and the test was repeated to further reduce mechanical losses. The results of this test suggest that the efficiency has improved.

CHAPTER VI
CONCULUSION AND FUTURE WORKS

Advances in motor technology have made it easier to manufacture efficient motors, so it is necessary to design induction motors as high efficiency motors. International regulations prohibit the use of IE2 and IE3 efficiency class motors, making it necessary to design and manufacture high-efficiency IE4 class motors. The aim of this thesis is to analyze and mathematically calculate high-efficiency motors using computer-aided programs. The study analysed reference models of the standard IE2 efficiency class motor produced by the company. The difference between the analysed induction motor and the production model was clearly observed.

In the second step of the study, improvements were made using different designs. After creating the reference motor model, efficiency improvements were made by observing the difference between parameter changes one by one. Although previous studies have focused on designs that improve efficiency based on a single parameter, this thesis study reveals that a common design approach is more effective. The materials have been improved, and new stator and rotor slots designs, winding designs, and geometric dimensioning have been implemented. The designed motor models were produced and tested for optimal performance. The motor was sent to the Turkish Standards Institute motor laboratory for testing. The tests were repeated twice and the final result was obtained. Upon comparison of the tests, it was found that the motors were produced at the intended and designed IE4 efficiency level. electric motors with 132 kW, 160 kW, and 185 kW power, which were not included in the thesis but were tested, were found to be at IE4 efficiency level after the necessary winding designs were made using the same moulds. To produce efficient motors, it is important to reduce material losses by using advanced material technologies. For instance, more efficient sheet metal can be used instead of standard sheet metal, and bearings with less losses can be used instead of those with high losses. In the future, electric motor technology can be applied to various fields. To improve motor efficiency, it is recommended to study the use of magnet technology, optimal magnet

and material design, and lightweight motor technology for aviation and defence industries.

REFERENCES

[1] GALLEGO A. Rodriguez (2014), *Design and Optimization of an IE4, 4-pole, 7.5 kW Induction Motor* (Master's Thesis), Royal Institute of Technology, Stockholm.

[2] MIDDELBERG R. Leo (2011), "Energy Efficient Electric Motors Some Caveats to Their Use", *In, Proceedings of the 8th Conference on the Industrial and Commercial Use of Energy,* pp. 93-99, Cape Peninsula University of Technology, Cape Town, South Africa.

[3] PETER Ioan (2012), "Induction Motors with Squirrel Cage Rotor, with IE2 Efficiency Level, up to 18.5 kW. Methods for Increasing the Efficiency", *13th International Conference on Optimization of Electrical and Electronic Equipment (OPTIM),* pp. 550,556, Brasov, Romania.

[4] SHUMEI Cui, YING Dai and LIWEI Song (2006), "Rotor Slots Design of Induction Machine for Hybrid Electric Vehicle Drives", *In, 2006 IEEE Vehicle Power and Propulsion Conference*, pp. 1-3, Windsor, UK, DOI: 10.1109/VPPC.2006.364375.

[5] MAKHETHA Eveline, MUTEBA Mbika and NICOLAE Dan Valentin (2019), "Effect of Rotor bar Shape and Stator Slot Opening on the Performance of Three Phase Squirrel Cage Induction Motors with Broken Rotor Bars", *In, 2019 Southern African Universities Power Engineering Conference/Robotics and Mechatronics/Pattern Recognition Association of South Africa (SAUPEC/RobMech/PRASA),* pp. 463-468, Bloemfontein, South Africa, DOI:10.1109/RoboMech.2019.8704850.

[6] HUANG Yuanfeng and WANG Haifeng (2016), "Loss Calculation of Asynchronous Frequency Conversion Motor with Cast Copper Rotor", *In, 2016 19th International Conference on Electrical Machines and Systems (ICEMS),* pp. 1-4, Chiba, Japan.

[7] ASHWIN D, ASHOK S, DIXIT Manglesh and CHAVAN Vinila (2015), "Design Optimization of 15 kW, 2-Pole Induction Motor to Achieve IE4 Efficiency Level with Copper Die-Casting", *In, Proceedings of IEEE International Conference on Technological Advancements in Power and Energy, TAP Energy*, pp. 98-102, Kollam, India, DOI:10.1109/TAPENERGY.2015. 7229599.

[8] REN Ziyan, ZHANG Dianhai and KOH Chang (2013), "A New Sensitivity-Based Reliability Calculation Algorithm in the Optimal Design of Electromagnetic Devices", *Journal of Electrical Engineering and Technology*, Vol. 8, No. 2, pp. 331-338, DOI:10.5370/JEET.2013.8.2.331.

[9] SARAVANAN C, AZARUDEEN A, Mohamed and SELVAKUMAR S. (2012). "Performance of Three Phase Induction Motor Using Modified Stator Winding", *Global Journal of Researches in Engineering Electrical and Electronics Engineering*, Vol. 12, No. 5, p. 1.

[10] ION C. Petrea and PETER Ioan (2022), "Manufacturing of IE4 Induction Motors", *2022 IEEE 20th International Power Electronics and Motion Control Conference (PEMC)*, pp. 373-377, Brasov, Romania. DOI:10.1109/PEMC 51159.2022.9962846.

[11] JIA Shaofeng, ZHANG Ping, LIANG Deilang, DAI Maocun and LIU Jinjun (2019), "Design and Comparison of Three Different Types of IE4 Efficiency Machines", *2019 22nd Int. Conf. Electr. Mach. Syst. ICEMS 2019*, pp. 2019-2022, Harbin, DOI: 10.1109/ICEMS.2019.8921786.

[12] KAZMIERKOWSKI P. Marian (2020), "Induction Machines Handbook", *IEEE Industrial Electronics Magazine*, Vol. 14, No. 4, pp. 185-186.

[13] WIKIPEDIA (2023), *Main Page*, https://en.wikipedia.org/wiki/, DoA. 2.12.2023.

[14] MMR (2023), *Electric AC Motors Market: Global Industry Analysis and Forecast (2023-2029)*, https://maximizemarketresearch.com/market-report/global-electric-ac-motors-market/97113/, DoA. 2.12.2023.

[15] CEPOI Radu, SZABO Lorand and FLORINA Jașcău (2017), "Current Trends in Energy Efficient Electrical Machines", *Journal of Electrical and Electronics Engineering*, No. 10, pp. 13-18.

[16] SARIOĞLU M. Kemal, BOĞOSYAN Seta and GÖKAŞAN Metin (2003), *Asenkron Makinalar ve Kontrolü*, Birsen Yayınevi, İstanbul.

[17] SARIOĞLU M. Kemal (1983), *Elektrik Makinalarının Temelleri Asenkron Makinalar,* Çağlayan Kitabevi, İstanbul.

[18] CHAPMAN J. Stephen (2005), *Electric Machinery Fundamentals,* Fourth Edition, McGraw-Hill, New York.

[19] FITZGERALD Arthur E., KINGSLEY. Charles and UMANS D. Stephen (2014), *Elektrik Makineleri,* Trans. GÜRLEYÜK Sırrı Sunay, Palme Yayıncılık, Ankara.

[20] SAÇKAN A. H. (1994), *Asenkron Motorlar,* Birsen Yayınevi, İstanbul.

[21] TÜRK STANDARDLARI ENSTİTÜSÜ (2012), TS EN 60034-30 *Döner Elektrik Makinaları- Bölüm 30: Tek Hız Kademeli, Üç Fazlı Kafesli Endüksiyon Motorlarının Verimlilik Sınıfları* (IE Kodu).

[22] DAENOTES (2023), *Losses and Power Stages in Induction Motor,* www.daenotes.com, DoA. 2.12.2023.

[23] CIRCUIT GLOBE (2023), *Power Flow Diagram and Losses of Induction Motor,* www.circuitglobe.com, DoA. 2.12.2023.

[24] LINKEDIN (2023), *How to Reduce Core Losses in Induction Motors,* www.linkedin.com, DoA. 2.12.2023.

[25] ELECTRICAL TECHNOLOGY (2023), *Losses in a Motor- Power Stages in an Induction Motor,* www.electricaltechnology.org, DoA. 2.12.2023.

[26] OSWOS (2023), *Losses in Electric Motors Complete Overview,* https://oswos.com/motor-losses/, DoA. 2.12.2023.

[27] ELECTRICAL 4 U (2023), *Losses and Efficiency of Induction Motor,* www.electrical4u.com, DoA. 2.12.2023.

[28] AARNIOVUORI Lassi, NIEMELÄ Markku, PYRHÖNEN Juha, CAO Wenping and AGAMLOH Emmanuel B. (2018), "Loss Components and Performance of Modern Induction", *ICEM 2018 Organizing Committees,* pp. 1253-1259, Alexandroupoli.

[29] PYRHONEN Juha, JOKINEN Tapani and HRABOVCOV´a Valeria (2008), *Design of Rotating Electrical Machines,* John Wiley & Sons, Chichester.

[30] KOCA Y. Bahadır and ÜNSAL Abdurrahman (2017), "Asenkron Motor Arızalarının Değerlendirilmesi", *Teknik Bilimler Dergisi,* Vol. 7, No. 2, pp. 37–46, https://dergipark.org.tr/tr/pub/tbed/issue/30206/300598, DoA. 3.7.1017.

[31] JANSSENS M. (2009), “SKF Energy Efficient Deep Slot Ball Bearings for Higher Driveline Efficiency”, *In, Proceedings of the 6th International Conference EEMODS,* Eds. Paolo Bertoldi and Constantin Bogdan Atanasiu, p. 9, Publications Office of the European Union, Nantes.

[32] BRUNNER Conrad U. (2023), *Electric Motors,* https://www.iec.ch/government-regulators/electric-motors, DoA. 10.12.2023.

[33] MENZEL MOTORS (2023), *IEC Motors*, https://www.menzel-motors.com/iec-motors, DoA. 1.02.2024.

[34] BRUNNER Conrad U. (2023), *Electric Motors,* https://www.iec.ch/government-regulators/electric-motors, DoA. 10.12.2023.

[35] KESKİN ARABUL Fatma, SENOL Ibrahim and ONER Yasemin (2020), “Performance Analysis of Axial-Flux Induction Motor with Skewed Rotor”, *Energies*, Vol 13, No. 19, pp. 4991, DOI: 10.3390/EN13194991.

[36] UL (2023), *Global Market Access Regulatory News Update*, https://www.ul.com/resources/global-market-access-regulatory-news-update, DoA. 10.12.2023.

[37] RAJINI V. and NAGARAJAN V. S. (2018), *Eletrical Machine Design*, Pearson Education India, Noida.

[38] NAWAZISH Ali S., HANIF Athar and AHMED Qaader (2016), “Review in Thermal Effects on the Performance of Electric Motors”, *2016 International Conference on Intelligent Systems Engineering (ICISE)*, pp. 83-88, Islamabad.

[39] HANIF Athar, NAWAZISH Ali S., AHMED Qadeer and BHATTI Aamir (2016), “Effect of Variation in Rotor Resistance on the Dynamic Performance of Induction Motor”, *2016 35th Chinese Control Conference (CCC),* pp. 9524-9529, Chengdu.

[40] KERKMAN Russel, SEIBEL Brian, ROWAN Tim A. and SCHLEGEL David (1996), “New Flux and Stator Resistance Identifier for AC Drive Systems*”, IEEE Transactions on Industry Applications*, Vol. 32, No. 3, pp. 585-593, DOI:10.1109/28.502170.

[41] MARINO R., PERESADA S. and TOMEI P. (2000), “On-line Stator and Rotor Resistance Estimation for Induction Motors”, *IEEE Transactions on Control Systems Technology*, Vol. 8, No. 3, pp. 570-579.

[42] SALOMON C. P., SANT'ANA W. C., BORGES da SILVA L. E., LAMBERT-TORRES G., BONALDI E. L., de OLIVEIRA L. E. L. and BORGES da SILVA J. G. (2015), "Induction Motor Efficiency Evaluation Using a New Concept of Stator Resistance", *IEEE Transactions on Instrumentation and Measurement*, Vol. 64, No. 11, pp. 2908-2917.

[43] KARANAYIL Baburaj and RAHMAN M. Fazlur (2007), "Online Stator and Rotor Resistance Estimation Scheme Using Artificial Neural Networks for Vector Controlled Speed Sensorless Induction Motor Drive", *IEEE Transactions on Industrial Electronics*, Vol. 54, No. 1, pp. 167-176, DOI:10.1109/TIE.2006.888778.

[44] AKHTAR Junaid and BEHERA R. Kumar (2019), "Optimal Design of Stator and Rotor Slot of Induction Motor for Electric Vehicle Applications", *ET Electrical Systems in Transportation*, Vol. 9, No. 1, pp. 35-43, DOI:10.1049/iet-est.2018.5050.

[45] YU Xing and DUNNIGAN Matthew. A. (2002), "Novel Rotor Resistance Identification Method for an Indirect rotor Flux-Orientated Controlled Induction Machine System", *IEEE Transactions on Power Electronics*, Vol. 17, No. 3, pp. 353,364. DOI:10.1109/TPEL.2002.1004243.

[46] PARK Hyung, HONG Hyeon and LEE Ki-Doek (2022), "Study on a Design Considering the Transient State of a Line-Start Permanent Magnet Synchronous Motor Satisfying the Requirements of the IE4 Efficiency Class", *Energies*, Vol. 15, No. 24, p. 1-14, DOI:10.3390/en15249644.

[47] KIRTLEY James, SCHIFERL Richard, PETERS Dale and BRUSH, Edwin (2009), "The Case for Induction Motors with Die-cast Copper Rotors for High Efficiency Traction Motors", *SAE World Congress & Exhibition*, Detroit Michigan, DOI:10.4271/2009-01-0956.

[48] CAVAGNINO Aandrea, VASCHETTO Silvio and FERRARIS Luca (2018), "Towards an IE4 Efficiency Class for Induction Motors with Minimal Manufacturer Impact", 2018 *IEEE Energy Conversion Congress and Exposition (ECCE)*, pp. 289-296, Portland, DOI:10.1109/ECCE.2018.8557586.

[49] De ALMEID Anibal and FERREIRA Fernando (2013), “Beyond Induction Motors—Technology Trends to Move up Efficiency”, *49th IEEE/IAS Industrial & Commercial Power Systems Technical Conference*, pp. 1-13, Stone Mountain, DOI: 10.1109/ICPS.2013.6547330.

[50] CAVAGNINO Andrea, VASCHETTO, Silvio and FERRARIS, Luca (2020), “Striving for the Highest Efficiency Class with Minimal Impact for Induction Motor Manufacturers”, *IEEE Transactions on Industry Applications*, Vol. 56, No. 1, pp. 194-204, DOI:10.1109/TIA.2019.2949262.

[51] LIANG Daniel and ZHOU Victor (2018), “Recent Market and Technical Trends in Copper Rotors for High-Eficiency Induction Motors”, *2018 International Power Electronics Conference (IPEC-Niigata 2018 -ECCE Asia)*, pp. 1943-1948, Niigata, Japan, DOI:10.23919/IPEC.2018.8507879.

[52] JAŻDŻYŃSKI Wieslaw (2011), *Modeling and Optimization of an IE4-Class High-Efficiency Induction Motor Prototype*, https://yadda.icm.edu.pl/baztech/element/bwmeta1.element.baztech-article-BPS2-0062-0044/c/Jazdzynski_ME_5_93__37-42.pdf, DoA. 2.12.2023.

[53] ASHWIN D., ASHOK S. and DIXIT M. (2015), “Design Optimization of 15 kW, 2-Pole Induction Motor to Achieve IE4 Efficiency Level with Copper Die-Casting”, *2015 International Conference on Technological Advancements in Power and Energy (TAP Energy)*, pp. 98-102, Kollam, DOI: 10.1109/TAPENERGY.2015.7229599.

[54] JIA Shaofeng, ZHANG Ping, LIANG Deliang and DAI Maocun (2019), “Design and Comparison of Three Different Types of IE4 Efficiency Machines”, *2019 22nd International Conference on Electrical Machines and Systems (ICEMS)*, pp. 1-4, Harbin. DOI: 10.1109/ICEMS.2019.8921786.

[55] GOMAN Victor, PRAKHT Vladimir, KAZAKBAEV Vadim and DMITRIEVSKII Vladimir (2020), “Comparative Study of Induction Motors of IE2, IE3 and IE4 Efficiency Classes in Pump Applications Taking into Account CO2 Emission Intensity”, *Appl. Sci.*, Vol. 10, No. 23, p. 8536. DOI:10.3390/app10238536.

[56] JAŻDŻYŃSKI Wieslaw (2011), *Modeling and Optimization of an IE4-Class High-Efficiency Induction Motor Prototype*, https://yadda.icm.edu.pl/baztech/element/bwmeta1.element.baztech-article-BPS2-0062-0044/c/Jazdzynski_ME_5_93__37-42.pdf, DoA. 2.12.2023.

[57] ASHWIN D, ASHOK S, DIXIT Manglesh and CHAVAN Vinila (2015), "Design Optimization of 15 kW, 2-Pole Induction Motor to Achieve IE4 Efficiency Level with Copper Die-Casting", *In, Proceedings of IEEE International Conference on Technological Advancements in Power and Energy, TAP Energy*, pp. 98-102, Kollam, India, DOI:10.1109/TAPENERGY.2015. 7229599.

[58] CAVAGNINO Aandrea, VASCHETTO Silvio and FERRARIS Luca (2018), "Towards an IE4 Efficiency Class for Induction Motors with Minimal Manufacturer Impact", 2018 *IEEE Energy Conversion Congress and Exposition (ECCE),* pp. 289-296, Portland, DOI:10.1109/ECCE.2018.8557586.

[59] DORRELL David (2014), "A Review of the Methods for Improving the Efficiency of Drive Motors to meet IE4 Efficiency Standards", *Journal of Power Electronics,* Vol. 14, No. 5, pp. 842-851.

[60] KIM Min, PARK Jung, LEE Kyu and LEE Sung (2022), "Performance Characteristics of the Rotor Conductor of an IE4 Class Induction Motor with Varying Al-Cu Ratio", *IEEE Transactions on Magnetics,* Vol. 58, No. 8, p. 8203406, DOI:10.1109/TMAG.2022.3153335.

[61] MUÑOZ TABORA Jonathan, de LIMA TOSTES Maria and ORTIZ de MATOS Edon (2020), "Voltage Harmonic Impacts on Electric Motors: A Comparison Between IE2, IE3 and IE4 Induction Motor Classes", *Energies,* Vol. 13, No. 13, p. 3333, DOI:10.3390/en13133333.

[62] LIU Huai, KIM In-Gun, JEONG Je-Myung and LEE Ju (2016), "Study on the High Efficiency Design of IE4 Synchronous Reluctance Motor Replacing IE3 Induction Motor", *The Transactions of The Korean Institute of Electrical Engineers,* Vol. 65, No. 3, pp. 411-418, DOI:10.5370/KIEE.2016.65.3.411.